Ionospheric flows relating to transpolar arc formation

R. C. Fear and S. E. Milan

29th September 2012

An edited version of this paper was published by AGU.

Citation: Fear, R. C. and Milan, S. E. (2012), Ionospheric flows relating to transpolar arc formation, *J. Geophys. Res.*, **117**, A09230, doi:10.1029/2012JA017830.

Department of Physics & Astronomy, University of Leicester, Leicester, LE1 7RH, United Kingdom

Correspondence to: r.fear@ion.le.ac.uk

Abstract

Transpolar arcs are large-scale auroral features which are observed within the polar cap when the IMF has a northward component. One leading candidate formation mechanism proposes that they are formed by reconnection in the magnetotail some time after a period of dayside reconnection with a non-zero IMF B_Y component which introduces a twist into the magnetotail. As a result of the twist, the mechanism predicts that the return flows of the newly-closed magnetic field lines are asymmetric about midnight; their direction should depend upon the IMF B_Y component in the hours beforehand, and should be opposite in the northern and southern hemispheres. In this paper, we use data from the SuperDARN network of high-latitude ionospheric radars to examine whether such ionospheric flows are present before the formation of 33 transpolar arcs. We find that the flows are present and in a manner that is consistent with the reconnection mechanism for 76% of the events; in the remaining few, the discrepancy can be attributed either to an uncertainty in the formation time determined for the arc (due to previous polar cap activity in the same local time sector) or due to the geometry of the radars which observe the backscatter.

1 Introduction

The main region of auroral emission at Earth is the auroral oval, which lies on closed magnetic field lines. The auroral oval in each hemisphere encircles the polar cap, which is the region of open magnetic flux which maps out into the magnetotail lobes. When the interplanetary magnetic field (IMF) is northward, high latitude auroras are sometimes observed within the polar cap; early ground-based observations revealed that these auroral forms are often aligned in the direction of the Sun (*Mawson*, 1925; *Weill*, 1958). Consequently they are variously referred to as high latitude auroras, polar cap arcs or Sun-aligned arcs. It has been shown that the occurrence of high latitude auroras correlates with periods of low magnetic activity (*Davis*, 1963) and northward IMF (*Berkey et al.*, 1976; *Gussenhoven*, 1982). The advent of global-scale imaging of the polar region revealed that high latitude auroras can also occur on a large scale. Such auroral forms are called transpolar arcs; they form on the night side of the auroral oval, but at times they can extend through to the day side of the oval, in which case they are also called 'theta aurora' (*Frank et al.*, 1982).

There are some similarities between the smaller-scale arcs that are often observed by sensitive all-sky imagers, or from low Earth orbit, and global-scale transpolar arcs. Both sets of arcs are typically Sun-aligned (*Mawson*, 1925; *Frank et al.*, 1982), and their motion appears to depend upon the circulation of flux caused by lobe reconnection, and therefore depends on both the IMF B_Y component and the location of the arc (*Craven et al.*, 1991; *Valladares et al.*, 1994; *Kullen et al.*, 2002; *Milan et al.*, 2005; *Hosokawa et al.*, 2011). However, there are also observational differences – there is no significant reported dependence on the IMF B_Y component of the location at which small-scale arcs form (*Valladares et al.*, 1994), whereas the location at which transpolar arcs form depends upon the longer-term history of B_Y (*Fear and Milan*, 2012). The source region and magnetic field topology for these two types of arc may also be different (*Shinohara and Kokubun*, 1996; *Carlson and Cowley*, 2005); the plasma precipitation observed above transpolar arcs is consistent with a plasma sheet origin, implying that transpolar arcs occur on closed field lines (*Peterson and Shelley*, 1984; *Frank et al.*, 1986), whereas *Carlson and Cowley* (2005) found that weaker-intensity Sun-aligned arcs could be formed by accelerated polar rain and could therefore occur on open magnetic field lines.

Several mechanisms have been proposed to explain the formation of transpolar arcs, which have been reviewed by *Zhu et al.* (1997) and also summarized recently by *Fear and Milan* (2012). The mechanisms vary considerably. In some, the arcs are thought to be formed by field-aligned current systems which are driven by the ionospheric convection cells which form when the IMF is northward (e.g. *Chiu et al.*, 1985; *Lyons*, 1985). *Makita et al.* (1991) proposed that the arcs could be an extension of the main oval, caused by a thickening of the oval on either the dawn or dusk side due to a tilted plasma sheet or a dawn-dusk asymmetry in the thickness of the plasma sheet. Two proposed mechanisms (*Kullen*, 2000; *Milan et al.*, 2005) require the introduction of a twist into the magnetotail, which is observed when the IMF has a significant B_Y component (*Fairfield*, 1979). Under these conditions, the B_Y component can be introduced into the magnetotail by one of two mechanisms. If the IMF is southward or moderately northward, dayside reconnection can occur, in which case the newly-opened magnetic field lines experience a magnetic tension with a component away from local noon. Consequently, flux is added to the magnetotail in an asymmetric manner about the noon/midnight plane, and a B_Y component is introduced into the lobe, twisting the magnetotail (*Cowley*, 1981). This component remains present even if the IMF subsequently turns northward, and is eventually introduced onto closed magnetic field lines when lobe flux closes to form the plasma sheet (*Cowley*, 1981). Alternatively, a B_Y component can be introduced via the 'stirring' of flux which occurs when single lobe reconnection occurs when the IMF is northward (*Russell*, 1972; *Reiff and Burch*, 1985). *Kullen* (2000) modeled the effect of such a rotation, introducing it into the *Tsyganenko* (1989) model as a perturbation at the Earthward end of the magnetotail, and propagating the planar rotation front tailwards. They then found that if magnetic field lines from the distant plasma sheet were mapped to the ionosphere, a feature resembling a transpolar arc was formed on the dawn or dusk side (depending on the sign of B_Y) and moved across the polar cap as the rotation front was propagated tailward. (Note also that the *Kullen* (2000) model only describes arcs which form at the dawn or dusk side and move across the polar cap, whereas the *Makita et al.* (1991) model only describes arcs which form on the dawn or dusk side of the oval and remain there.)

Milan et al. (2005) presented observations of the formation of a transpolar arc, including global-scale UV images of the polar cap and radar observations of the ionospheric flow both within the polar cap and co-located with the auroral oval. They proposed an alternative mechanism (sketched in Figure 1) in which

the arc was formed by night side reconnection in a twisted magnetotail. The introduction of the twist either occurs during an earlier period of dayside reconnection when the IMF has a strong B_Y component and is either southward or moderately northward, or is introduced by an earlier period of single lobe reconnection when the IMF is northward. The arc itself is formed later when the IMF is northward, suppressing dayside reconnection, but the B_Y component of lobe field lines that have already been opened by dayside reconnection or reconfigured by single lobe reconnection remains unchanged (but by which time the field lines have moved such that they are adjacent to the plasma sheet). Consequently, when magnetotail reconnection occurs (Figure 1b), the northern and southern hemisphere footprints of newly closed magnetic field lines straddle the midnight meridian (*Cowley*, 1981). The return flow of the closed flux then becomes more complicated than originally envisaged by *Dungey* (1961). In order for a field line to return to the dayside, one footprint has to move faster than the other, towards and past midnight MLT, to 'catch up' with its counterpart in the other hemisphere, giving rise to azimuthal flows in the ionosphere that are asymmetric about midnight MLT (*Grocott et al.*, 2003), shown in Figure 1c. The locations of the footprints which have further to travel are determined by the twist in the magnetotail, and hence by the earlier IMF B_Y component; the locations are also mirrored about midnight in opposite hemispheres. If the IMF B_Y component was negative in the hours beforehand (and hence the B_Y component in the inner lobe is currently negative, which is the case sketched in Figure 1b & c) then the flows will be directed from the post-midnight sector towards earlier local times (i.e. westward) in the northern hemisphere and eastward from the pre-midnight sector in the southern hemisphere (*Grocott et al.*, 2003). The opposite directions are observed if B_Y was positive beforehand (*Grocott et al.*, 2004). *Milan et al.* (2005) proposed that the return flow of field lines which cross the plasma sheet near midnight is prevented as the northern and southern halves of the field lines experience opposing forces in the dawn/dusk direction, and hence the field line as a whole experiences no net dawn/dusk component of force. This results in a build up of closed flux. As the closed field lines in the magnetotail contract and further reconnection takes place, the footprints of the closed field lines that cross the plasma sheet near midnight protrude into the polar cap, forming the transpolar arc (Figure 1b & c). This mechanism predicts that the location of the arc should depend upon the hemisphere and the B_Y component in the inner lobe, adjacent to the plasma sheet (and consequently on the IMF orientation several hours earlier, when the inner lobe magnetic field line was first opened). If $B_Y > 0$, the arc should form pre-midnight in the northern hemisphere and post-midnight in the southern hemisphere; if $B_Y < 0$ (the case shown in Figure 1b & c) then the arc should form post-midnight in the north and pre-midnight in the south. In both cases, its subsequent motion is caused by the 'stirring' of flux by lobe reconnection, and therefore depends on the current IMF orientation. In this mechanism, the magnetic field lines threading the TPA are closed field lines which are embedded within the open field lines that constitute the polar cap and lobe.

The *Milan et al.* (2005) mechanism leads to four key predictions. First, the magnetic local time at which transpolar arcs form should depend upon the IMF B_Y component. Second, the dependence upon the IMF B_Y component should be delayed by several hours, as the arc location depends in the first instance upon the B_Y component in the inner lobe, adjacent to the plasma sheet, which is dictated by the IMF orientation several hours earlier when that field line was first opened at the dayside (*Dungey*, 1961; *Cowley*, 1981; *Milan*, 2004). Third, the magnetic local times at which arcs form should be mirrored about midnight in opposite hemispheres. Fourth, the initial emergence of the arc from the main auroral oval should be preceded by asymmetric ionospheric flows of the type reported by *Senior et al.* (2002) and *Grocott et al.* (2003, 2004), directed from the magnetic local time at which the arc subsequently first emerges, towards and across midnight MLT (Figure 1).

In terms of the first three predictions, there have been some conflicting results in the past. Early statistical studies used either ground-based imaging or spacecraft imagers with relatively small fields of view. *Gussenhoven* (1982) found a weak tendency for northern hemisphere polar cap arcs to occur post-midnight when B_Y was negative and pre-midnight when B_Y was positive, and *Gusev and Troshichev* (1986) found the opposite tendency in hook-shaped sun-aligned arcs which were observed on the day side of the southern hemisphere polar cap. Both observations are consistent with the *Milan et al.* (2005) mechanism (and others – see discussion in *Fear and Milan* (2012)), but in both cases the IMF was evaluated in the hour or two before the arc was observed. However, a subsequent study by *Valladares et al.* (1994) has found no significant correlation between B_Y and the location of polar cap arcs. The aforementioned studies were carried out using observations from the ground or low-altitude spacecraft. *Kullen et al.* (2002) carried out the first statistical study of truly transpolar arcs, that were imaged on a global scale. They examined the correlation between the local time at which northern hemisphere

arcs occurred and the IMF B_Y component during the lifetime of the arc. They concluded that it was necessary to divide the arcs into several different classes: (a) arcs which formed on the dawn or dusk side of the polar cap and moved across the polar cap, (b) arcs which formed on the dawn or dusk side and did not move, (c) arcs which formed in the midnight sector (with or without subsequent motion), (d) 'bending' arcs, where the sunward end of the arc separated from the main oval and moved into the polar cap whilst the antisunward end remained fixed, and (e) multiple simultaneous arcs. They found that three different mechanisms (proposed by *Makita et al.* (1991), *Rezhenov* (1995) and *Kullen* (2000)) were necessary to explain classes (a-c). They noted in particular that nine out of the eleven 'moving' arcs (category a) were associated with a change in the IMF B_Y component in the hour preceding the arc's first observation, and concluded that these arcs were triggered by the sign change (*Kullen*, 2000).

In a recent paper (*Fear and Milan*, 2012), we have presented a statistical study of the IMF control of 131 transpolar arcs observed by the IMAGE satellite. In order to distinguish between IMF control of the initial location of transpolar arcs and IMF control of their subsequent motion, we only included arcs if their initial formation was observed by IMAGE. (If an arc forms during a significant data gap, then it may move considerably by the time it is first observed and hence its initial local time is uncertain.) The mechanism proposed by *Milan et al.* (2005) links the initial location of a transpolar arc with the B_Y component in the inner lobe (adjacent to the plasma sheet), which in turn depends upon the IMF B_Y component several hours beforehand (*Dungey*, 1961; *Cowley*, 1981). In order to examine whether any correlation between the IMF B_Y component and the initial local time of transpolar arcs is delayed by the timescales that are implied by the Dungey cycle, we examined the IMF over several hours before and after the initial emergence of each arc into the polar cap. It was found that the strongest correlation between B_Y and location occurred when the B_Y component was measured $\sim$4 hours before the arc was first observed. This delay is consistent with the timescales that are expected for the passage of a newly-opened magnetic field line on the dayside to a position adjacent to the plasma sheet, as can be deduced from the results of *Dungey* (1961), *Borovsky et al.* (1993) and *Milan et al.* (2007). (See *Fear and Milan* (2012), particularly Figure 1, for further discussion of this point.) No clear division was present between dawn- or dusk-side arcs and midnight-sector arcs, as there was a continuous distribution across local time. The same $\sim$4 hour delay was found for arcs which subsequently moved as for stationary arcs. The correlation remained strong for several hours after the initial emergence of the stationary arcs, but rapidly reduced for moving arcs. This was interpreted as evidence that whereas the local time at which arcs formed was driven by the B_Y component several hours beforehand, their subsequent motion was driven by a much more prompt ionospheric response to lobe reconnection (*Milan et al.*, 2005). *Fear and Milan* (2012) concluded that the *Milan et al.* (2005) mechanism was capable of explaining the formation of both moving and stationary arcs at all local times. It was also concluded that the appearance in earlier studies of a B_Y 'trigger' for moving arcs was not a physical effect, but was a selection effect – the motion of an arc across the midnight sector requires a B_Y sign change at some point within the $\sim$4 hours prior to the formation of the arc or during the arc's lifetime due to the separate effects controlling the initial location and subsequent motion; if the sign change does not occur then the arc would still form, but would either remain stationary or move away from the midnight sector.

In this paper, we seek to test the fourth prediction of the *Milan et al.* (2005) mechanism by examining ionospheric flows present on closed magnetic field lines (i.e. coincident with the auroral oval) to see whether the asymmetric azimuthal flows discussed by *Grocott et al.* (2003, 2004) are present. Whilst several previous studies have examined the ionospheric flows present on the transpolar arcs after the arcs have formed (using either ionospheric radar data (e.g. *Nielsen et al.*, 1990; *Liou et al.*, 2005) or observations from low altitude spacecraft (e.g. *Frank et al.*, 1986; *Østgaard et al.*, 2003; *Cumnock and Blomberg*, 2004)), in this paper we consider only the ionospheric flows in the main auroral oval which precede the formation of the arc. In the following section, we provide an overview of the instrumentation used in this study and the survey carried out by *Fear and Milan* (2012). We then present observations of moderate or strong ionospheric flows preceding 27 of the transpolar arcs identified by *Fear and Milan* (2012) for which there were adequate observations of the ionospheric motions (including one arc where adequate observations were available in both the northern and southern hemispheres). We find that three quarters of the arcs are preceded by ionospheric flows which are consistent with the *Milan et al.* (2005) mechanism. The events which appear, at first sight, to be inconsistent with this mechanism are mostly explained by an uncertainty in the start time that was identified for each arc or by the lack of data from azimuthally-pointing radar beams. We then analyze a few extra cases where relatively weak flows are present, the majority of which are also consistent with the reconnection mechanism. Finally,

we discuss our results and draw conclusions in Sections 4 and 5.

2 Instrumentation and Survey

In this study, we use the 131 transpolar arcs that were identified by *Fear and Milan* (2012). The arcs were identified by examining auroral images from the Wideband Imaging Camera (WIC) and Spectrographic Imager 121.8 nm camera (SI12), which are part of the Far Ultra Violet (FUV) instrumentation on the IMAGE spacecraft (*Mende et al.*, 2000a,b,c). WIC is sensitive to emissions at wavelengths between 140 and 190 nm, whilst SI12 images a narrow band at 121.8 nm. SI12 images have a lower spatial resolution than WIC (at apogee, an SI pixel has a 92×92 km footprint, compared with 52×52 km on WIC), but images from both instruments are available at 2 minute cadence. Since SI12 is tuned to sample Doppler-shifted Lyman-α emissions, it is not sensitive to dayglow (unlike WIC).

IMAGE observed the northern hemisphere aurora between 2000-03, and the southern hemisphere between 2003-05. *Fear and Milan* (2012) examined images from both SI12 and WIC between June 2000 and September 2005, and identified transpolar arcs which satisfied three criteria: (1) the initial emergence of the arc from the auroral oval into the polar cap had to be observed by WIC and/or SI12; (2) arcs had to persist for at least 30 minutes and (3) an arc had to make a significant protrusion into the polar cap at some point in its lifetime. These criteria were chosen to ensure that the initial local time of the arc could be determined as accurately as possible, and to exclude other features such as the 'double oval' which is associated with the later stages of auroral substorms (e.g. *Elphinstone et al.*, 1995).

The ionospheric flow data are provided by the SuperDARN radar network (*Greenwald et al.*, 1995; *Chisham et al.*, 2007). SuperDARN is an array of high-latitude high-frequency radars which provides observations of the ionospheric flow in the northern and southern hemisphere auroral regions. Data from a single radar provides the line-of-sight velocity component, but a global two dimensional map of the ionospheric flows can be obtained using the map potential method (*Ruohoniemi and Baker*, 1998). This technique combines data from all available radars, supplemented by data from a statistical model to constrain the solution in regions where there is no data, to determine the distribution of the ionospheric electrostatic potential as an expansion of spherical harmonics. In most of Section 3, we use data that have been processed by the map potential method and show ionospheric velocity vectors that combine the line-of-sight component of the ionospheric flow observed by the radar(s) with a perpendicular component that is derived from the global electrostatic potential fit ('true' vectors as discussed by *Ruohoniemi and Baker* (1998)). In Section 3.3, we examine the line-of-sight velocity vectors directly for some events.

We also provide averaged values of the interplanetary magnetic field (IMF) B_Y component preceding all events, using data from the OMNI IMF data set, which is lagged to the bow shock as described by *King and Papitashvili* (2005).

3 Observations: Ionospheric flows

The *Milan et al.* (2005) mechanism predicts that prior to the first emergence of the transpolar arc into the polar cap, asymmetric azimuthal flows should be present and directed from the local time at which the arc subsequently emerges towards (and past) midnight MLT (Figure 1), opposite in direction to the flows that would arise from symmetric Dungey cycle convection cells. The enhanced flows should occur on closed magnetic field lines, and should therefore coincide with the auroral oval. Figure 1 also shows that a return flow of closed flux occurs on the opposite side of the arc (i.e. on the dawnward side of a post-midnight arc, or the duskward side of a pre-midnight arc); in this location, the flows are the same as expected in the symmetric Dungey cycle case. As the flows on the this side of the arc cannot be used to distinguish between the *Milan et al.* (2005) scenario and more common ionospheric flows, we do not use these flows as a test criterion although we do note their presence when observed.

In order to identify the presence or absence of asymmetric flows, we calculated the two dimensional flow patterns over the 30 minutes preceding the initial emergence of the arc into the polar cap, using the map potential procedure (*Ruohoniemi and Baker*, 1998). The SuperDARN radars typically each carry out a complete sweep of their fields of view every one or two minutes (depending upon the operating mode of each radar), but previously reported azimuthal flow bursts during intervals of northward IMF have lasted of the order of 10-15 minutes (*Grocott et al.*, 2003). Therefore, in order to acquire a simpler

view of the ionospheric behaviour on the timescale associated with these flows, we combined ten minute blocks of data. We then superimposed the 10 minute resolution map potential data on simultaneous auroral images provided by IMAGE in order to identify the flows that were present on closed magnetic field lines, and shortlisted events which had sufficient ionospheric backscatter to test the *Milan et al.* (2005) mechanism. All flows which occurred poleward of the auroral oval were ignored, as they occur on open magnetic field lines (i.e. they indicate the circulation of flux within the lobe).

Although each arc was observed in only one hemisphere, we examined the ionospheric flows in both hemispheres. The *Milan et al.* (2005) and *Grocott et al.* (2003, 2004) mechanisms predict that transpolar arcs and the related azimuthal ionospheric flows should occur in both hemispheres but mirrored about the noon/midnight meridian, which is consistent with simultaneous northern and southern hemisphere satellite observations of a transpolar arc reported by *Craven et al.* (1991) and with the opposite statistical dependency of the initial MLT on the IMF B_Y component that is observed in the northern and southern hemispheres (*Fear and Milan*, 2012). (We note in passing that *Østgaard et al.* (2003) has reported two cases where spacecraft observed both the northern and southern hemisphere polar caps, but a theta aurora was only observed in one hemisphere. Once formed, the motion of a pair of transpolar arcs can occur independently in each hemisphere if the rate of lobe reconnection differs between hemispheres (*Milan et al.*, 2005); due to uncertainties in the formation time of the arcs, or to data gaps, it is possible that arcs formed in both hemispheres in both cases reported by *Østgaard et al.* (2003) but the arc in one hemisphere moved to the edge of the polar cap such that it was indistinguishable from the main auroral oval (*Fear and Milan*, 2012).)

Two types of backscatter pattern were identified which allow the mechanism to be tested. In the first type, 'true' velocity vectors with a magnitude of at least 300 m s^{-1} (and hence a clear flow direction) were observed coincident with the auroral oval, between the initial magnetic local time of the arc and midnight MLT either as the arc first emerged or at some point in the preceding 30 minutes. The strength of these flows means that the flow direction is evident in the map potential vectors. In all of these cases, we checked whether the direction of the flow observed between the location at which the arc subsequently emerged and midnight MLT was consistent with the *Milan et al.* (2005) mechanism (i.e. directed towards midnight). In those cases where there was sufficient scatter to determine the dawnward or duskward edge of the flow channel (for post- and pre-midnight arcs respectively), we also checked whether this location coincided with the initial MLT of the arc. (This location will be referred to below as the 'dawnward or duskward' edge of the flow channel, although we use this to refer specifically to the edge that is on the same side of midnight as the initial location of the arc.) The ionospheric flows were identified as consistent with the mechanism if the flow direction and (where determined) the location of the dawnward or duskward edge of the flow channel was consistent with the mechanism at some point in the 30 minutes preceding the first emergence of the arc, and no contradictory flows (above 300 m s^{-1}) were observed in the remainder of this 30 minute period. If flows of at least 300 m s^{-1} were observed directed from midnight MLT towards the subsequent location of the arc at any stage in the 30 minute period, or the dawnward/duskward edge of the flow channel did not coincide with the location at which the arc formed (beyond a small change in the location as this indicates earlier variation of the IMF B_Y component) then the flows were classified as inconsistent. These 'moderate' or 'strong flow' events will be discussed in Sections 3.1 and 3.2.

In the second type of backscatter pattern, consistently weak 'true' velocity vectors were observed coincident with the auroral oval between the initial MLT of the arc and midnight MLT throughout the 30 minutes prior to the initial emergence of the arc. In order to establish whether there are any dawnward or duskward flows that can be used to test the *Milan et al.* (2005) mechanism, we examined the line of sight velocities observed by radars in the same local time sector as the arc initially formed. These 'weak flow' events will be discussed in Section 3.3. Detailed examination of the flows was not carried out for events where such weak flows were only observed in one or two of the 10 minute resolution maps in the half hour preceding the arc, since the lack of ionospheric backscatter in the other 10 minute map(s) means that the predicted flows could in principle be occurring unobserved at that time.

We consider first the 27 arcs which were preceded by ionospheric backscatter indicating flows on closed field lines that had a clear direction (i.e. the magnitude of the 'true' velocities exceeded 300 m s^{-1}), which are listed in Table 1. For one arc (TPA 34), such flows were present in both the northern and southern hemispheres; for simplicity in the following analysis, the flows in the northern and southern hemispheres will be treated as two separate events, making 28 arcs in total. The table lists the arc number (which is the reference number used in the supplementary material to *Fear and Milan* (2012)) and the time at

which the arc's protrusion into the polar cap was first identified. The third and fourth columns indicate whether there was sufficient scatter in the northern and/or southern hemispheres across the midnight sector and coincident with the main auroral oval to allow us to identify whether the formation of the arc is consistent with the *Milan et al.* (2005) mechanism or not. The final column denotes whether the arc was observed by the IMAGE spacecraft in the northern or southern hemisphere. In the following figures, arcs will be identified by both the arc number and the hemisphere from which the SuperDARN convection patterns are derived. The arcs used in this study and which have a number less than 100 were observed by IMAGE in the northern hemisphere, and those with a number greater than 100 were observed by IMAGE in the southern hemisphere (Table 1). Therefore, event '16S' refers to the transpolar arc which was observed on 22 January 2001 in the northern hemisphere and conjugate ionospheric flow data from the southern hemisphere. The arc observed on 18 October 2001 (TPA 34) had suitable ionospheric convection data in both hemispheres (denoted below as 34N and 34S). We also note that TPA 53 was the event studied by *Milan et al.* (2005). The arc studied by *Goudarzi et al.* (2008) (TPA 59 in the *Fear and Milan* (2012) survey) is not included in this paper; although fast flows indicative of magnetotail reconnection are observed duskward of the arc (which first forms pre-midnight), there is no scatter coincident with the auroral oval and between the arc & midnight MLT and so the mechanism cannot be tested using the procedure described above.

The ionospheric flows observed for these 28 events are summarised in Figures 2, 4 and 5, which contain:

- Events where the dawnward/duskward edge of the flow channel can be identified and both the flow direction and location of the edge of the flow channel are consistent with the location of the arc (Figure 2),
- Events where the flows observed between the location at which the arc subsequently emerges and midnight MLT are consistent with the *Milan et al.* (2005) mechanism, but there is insufficient scatter to identify the dawnward or duskward edge of the flow channel (Figure 4), and
- Events where either the direction of the flow or the location of the edge of the flow channel is inconsistent with the mechanism (Figure 5).

Each row in Figures 2, 4 & 5 shows two images which relate to a single event. The left-hand column shows an image of the arc between 30 and 64 minutes after it first emerged into the polar cap, to indicate the structure of the arc. The initial MLT of the arc is indicated by a pink or purple filled circle, with error bars which indicate the uncertainty in the determination of the MLT. (Both the MLT and its associated uncertainty are listed in the supplementary material to *Fear and Milan* (2012).) It is important to note that the initial MLT indicated in Figure 2 or 4 does not necessarily coincide with the location of the arc in the left-hand column, as the arc may have moved between its first emergence into the polar cap and the time plotted in the figure. The right-hand column shows an image of the auroral oval either at the time at which the arc first forms or up to 30 minutes beforehand, overlain by vectors representing the ionospheric flows averaged over the 10 minute period containing the auroral image. Each flow vector is denoted by a filled circle and a line; the flow is in the direction of the line away from the filled circle. The time of each auroral image and the time relative to the first emergence of the arc is indicated above each panel. The history of the IMF B_Y component is also indicated in each row; it is not trivial to determine exactly what time the magnetic field line that now forms the transpolar arc was first opened on the dayside, but we would expect this to be typically 3-5 hours earlier (*Fear and Milan*, 2012, and references therein). We have therefore indicated the sign of the average B_Y component observed in one-hour blocks centred 3, 4 and 5 hours before the time at which the arc was first observed.

In each of the 'consistent' events shown in Figures 2 and 4, we have shown the map potential data from the 10 minute period that contained either the strongest flows or the most extensive scatter. Other 10 minute periods in the 30 minutes preceding the arc might contain less scatter (caused by variation in the generation of ionospheric irregularities or their alignment relative to the radar beam) or weaker or stagnant flows (caused by the episodic nature of reconnection under these conditions (*Grocott et al.*, 2003, 2004)), but there are no cases in Figures 2 or 4 where strong flows occur at another point in the 30 minutes preceding the arc which contradict those predicted by the Milan et al. [2005] mechanism. Where observed, the precise location of the dawnward/duskward edge of the flow channel sometimes moves by up to 1 hour in MLT within the 30 minute period preceding the observed emergence of the

arc, indicating variation in the IMF B_Y component at the time that the newly-closed flux at the plasma sheet was first opened several hours earlier.

In all of the figures in this paper, the data are plotted on a magnetic latitude/magnetic local time grid with midnight at the bottom of the plot, dusk to the left and dawn to the right. Therefore the data are plotted as they would be viewed from above the northern hemisphere, and southern hemisphere data are plotted as they would be viewed from the north, through the planet. Furthermore, since transpolar arcs form at anti-conjugate locations in opposite hemispheres (that is to say, at locations that are mirrored about the midnight meridian), auroral images are reversed about the noon/midnight meridian in cases where the auroral image is being compared with ionospheric flows from the opposite hemisphere. For example, the image labelled TPA 34N (Figure 4) is compared with northern hemisphere flows and is plotted with a straightforward projection onto the MLT/magnetic latitude grid, since the IMAGE spacecraft observed the arc in the northern hemisphere, but for TPA 34S the same image is compared with southern hemisphere ionospheric data by reversing the auroral image about midnight (also Figure 4). Consequently, the initial MLT of TPA 34N is 4.5 MLT, whereas the initial MLT of TPA 34S (which is treated as a separate event) is 19.5 MLT.

3.1 Consistent moderate/strong flows

22 of the 28 arcs were preceded by consistent ionospheric flows in the 30 minutes prior to the first emergence of the arc into the polar cap. Figure 2 shows 12 events which are most clearly consistent with the *Milan et al.* (2005) mechanism, as the dawnward or duskward end of the flow channel is observed close to the location at which the arc subsequently emerges. In order to check the results of the map potential procedure, we also examined the line of sight velocity data used by each map in Figure 2; in all cases, evidence for the flow channel was observed in beams with an azimuthal component close to the dawnward or duskward edge of the flow channel (not shown), although the strength of the line-of-sight component depends upon the beam alignment relative to the flow channel. In several cases where radars had a largely poleward alignment in the same local time sector as the arc subsequently emerged, strong antisunward flows were also observed (visible in many of the map potential vectors in Figure 2 – e.g. TPA 92N). This is also consistent with the *Milan et al.* (2005) mechanism as it indicates the closure of flux in this local time sector and its exit from the polar cap (Figure 1c).

In all of the cases in Figure 2, there is an identifiable flow channel bounded by the initial MLT of the arc which subsequently forms, and with a flow directed from this location towards midnight MLT. This is highly consistent with the *Milan et al.* (2005) mechanism. In most cases, the flows coincide with the main part of the auroral oval, but in two cases (TPAs 6N & 57N), the enhanced flows occur coincident with a localised auroral brightening just poleward of the main oval. Since these flows do coincide with auroral emissions, we attribute them to the motion of newly closed field lines and include them in our discussion. Although we do not use the return of flux on the dawnward or duskward side of the arc for post- and pre-midnight arcs respectively as a test of the *Milan et al.* (2005) mechanism, these flows are also observed in several cases (TPAs 6N, 43N, 50N, 90N, and 92N).

The flow channel observed before TPA 39N is relatively weak, but this event has been included in Figure 2 because there is an identifiable flow channel between 1 and 2 MLT (with flows towards midnight MLT), and the eastward end of this flow channel coincides with the location at which the arc subsequently forms (2 MLT). These flow vectors are based on line-of-sight velocities of $\sim$250 m s^{-1} which are observed away from the Prince George radar in beams which have a significant westward component in this part of the field of view (not shown). Therefore, we are confident that these relatively modest flows are genuinely observed.

In most cases, the uncertainty of the initial MLT of the arc is relatively small ($\sim$ $\pm$1-2 hours of MLT). However, the initial MLT of TPA 50 has a large uncertainty (3 hours of MLT) which represents the atypical manner of the arc's evolution. Although the ionospheric flows observed in the northern hemisphere are not consistent with the precise value of the initial MLT (22 MLT), fast flows are observed across the midnight sector from 1 MLT (which is within the error bounds of the initial MLT estimate) past midnight towards 21 MLT (Figure 2). The evolution of TPA 50 is shown in more detail in Figure 3. Each pair of panels shows the same IMAGE observation, but the black and white image is overlaid with the ionospheric flows ('true' vectors) observed in the ten minutes following the time of the image. The initial MLT of the arc, along with its associated uncertainty, is indicated in each panel (22 $\pm$ 3 MLT). The initial MLT was identified as 22 MLT based on observations in the early stages of the arc's formation.

(At 10:10 and 10:30 UT, the arc can clearly be traced to the main auroral oval at 22 MLT.) Initially, the arc appears to 'peel off' from the auroral oval, but then at about 10:50 UT the end of the arc begins to protrude deeper into the polar cap, leading to a reverse 'L'-shaped arc. The bend in the arc occurs at 01 MLT, and the uncertainty in the initial MLT was chosen such that the bend and renewed protrusion into the polar cap occurred within the uncertainty range. The ionospheric flows associated with this event are changeable and complex, but fast flows on closed magnetic field lines (i.e. coincident with the main auroral oval) are observed between 1 MLT and midnight MLT from 09:30 to 10:10 UT (Figure 3). These flows are consistent with the *Milan et al.* (2005) mechanism if the arc forms at 1 MLT at 10:50 UT (i.e. if the formation of the arc is taken to be the protrusion of the 'L' radially into the polar cap, rather than the 'peeling' process which occurs between 09:50 and 10:30 UT).

The statistical link between the location at which transpolar arcs form and the longer-term history of the IMF B_Y component has been shown by *Fear and Milan* (2012), but we note that in ten of the twelve events shown in Figure 2, a the mean B_Y in at least one hour block was consistent with the *Milan et al.* (2005) mechanism prediction. (The prediction is that when the flux now forming the inner lobe was originally opened on the day side [approximately 4 hours earlier], B_Y should have been positive for pre-midnight arcs and negative for post-midnight arcs in the northern hemisphere, and vice versa for the southern hemisphere. In this context, the 'hemisphere' refers to the hemisphere of the SuperDARN scatter [i.e. to the 'N' or 'S' label in each panel], since the IMAGE images have been mirrored about midnight in cases where IMAGE and SuperDARN data come from opposite hemispheres. In light of the discussion of the flow pattern preceding TPA 50N, we have counted this event as a post-midnight arc, even though the MLT that was initially determined was pre-midnight.) In the case of TPA 53N, the B_Y components observed 3-4 hours beforehand were inconsistent with the location of the arc and the observed flow pattern, but no OMNI IMF data were available in the hour before that; it is not trivial to determine the exact time that the magnetic field lines now forming the TPA were first opened on the dayside, but it is possible that the IMF was not observed at this time. In the case of TPA 101N, the negative sign of B_Y in each hour block is also inconsistent with the observation of an arc which formed pre-midnight (but had moved post-midnight by the time it is shown in Figure 2) and the flow pattern associated with this arc, although this arc was formed very close to midnight MLT.

Figure 4 shows a further 10 events where the location of the dawnward/duskward end of the flow channel cannot be identified due to a lack of scatter in that region, but where the flow observed either in the midnight sector or at some point between the initial MLT of the arc and midnight MLT is consistent with the direction predicted by the *Milan et al.* (2005) mechanism. Although we cannot test whether the flow channel starts at the same location as the transpolar arc subsequently emerges for these events, we can confirm that asymmetric flows are present and that the available observations are consistent with the mechanism as far as they allow. In all cases in Figure 4, flows are observed in the direction from the initial location of the arc towards (and sometimes past) midnight MLT, either in the midnight sector or between midnight and the location of the arc. Again, we confirmed that flow patterns were observed in the original line of sight data that were consistent with those present in the map potential vectors.

The scatter for TPA 16S is restricted to a very local area at midnight MLT, and occurs poleward of what appears to be the main auroral oval. However, like TPAs 6N and 57N (Figure 2), these flows coincide with a brightening poleward of the main oval, which we take to indicate the fresh closure of further flux and hence we interpret these flows as on newly-closed magnetic field lines. Although the scatter for 16S is limited in extent, the dawnward flows observed at midnight MLT are due to a clear, but localised, patch of backscatter that is observed by the TIGER radar in beams which have a significant dawnward component (aligned by approximately 45° to the magnetic meridian). We are therefore confident that this event is consistent with the *Milan et al.* (2005) mechanism.

In several cases, there is a wide region without any backscatter between the arc and the observed dawnward/duskward flows (e.g. TPAs 17S, 34N, 34S, 70N, 73N), but again we emphasise that lack of scatter in these regions in no way contradicts the proposed mechanism, and the observed flows in the midnight sector are consistent with the mechanism.

In four cases (TPAs 34N, 64N, 70N, 73N), faster flows are observed on the opposite side of midnight from the location of the arc than the flows that are observed in the midnight sector. However, we point out first that this does not contradict the proposed mechanism, since there may be additional processes occurring closer to dawn/dusk, and secondly that it is also likely to be in part a consequence of the radar geometry. In each of these four cases, the 'true' vectors in the faster flow regions are dominated by the line-of-sight component rather than the potential fit component, whereas near midnight the line-of-sight

component of the 'true' vectors is weaker, indicating that near midnight the flows are more perpendicular to the radar beams and hence the velocities in these cases may be underestimates.

In all nine cases shown in Figure 4 for which IMF data were available, the sign of the B_Y component observed 3-4 hours before the arc was consistent with the location of the arc.

3.2 Apparently inconsistent moderate/strong flows

There are six arcs for which the ionospheric flows do not appear, on initial examination, to be consistent with the MLT at which the arc was identified by *Fear and Milan* (2012) as first emerging into the polar cap. These events are summarised in Figure 5, and will be discussed in this section. Most consist of events where ionospheric flows, coincident with the auroral oval, are directed from midnight MLT towards the initial MLT of the arc (contrary to the prediction of the reconnection mechanism), but two events (TPAs 111N & 123N) have flows that are in the expected direction but which start at a location which is either dawnward or duskward of the initial MLT of the arc. In the remainder of this section, we discuss two issues which may explain the discrepancy between the observed flows and those expected from the reconnection mechanism: uncertainty in the start time of the arc, and radar geometry.

3.2.1 Timing uncertainty

The analysis above was carried out using the arc formation time and location (in MLT) that was identified by *Fear and Milan* (2012) and listed in the supplementary material to that paper. However, further examination of four of the transpolar arcs reveals the presence of similar features in the hours beforehand at the same local time, indicating a greater uncertainty in the initial time determined for the arc. An example is shown in Figure 6, which shows several images before and after the time that was identified as the initial emergence of TPA 89 (17 December 2002, 14:08 UT). The top-left panel shows the auroral emissions observed by the IMAGE WIC camera at 09:40 UT, as the spacecraft emerged from perigee. The pink circle and error bar in each panel show the magnetic local time at which the arc was subsequently identified to form (at 14:08 UT). Although the precise morphology of the aurora at this time is unclear due to the viewing angle from the spacecraft, there appear to be emissions present poleward of the main auroral oval at about 03 MLT. This develops into a polar cap feature which might have been identified as a transpolar arc in our list had it not been visible in the first frame after perigee, making the determination of the arc's start time impossible (not shown). The second panel (top-right) shows the auroral emissions and ionospheric flows observed in the northern hemisphere a little while later. The flows are averaged over the interval 11:20–11:30 UT, and the image was taken at 11:20 UT. By this time, the arc has faded somewhat, but flows of $\sim$600 km s^{-1} are observed coincident with the auroral oval, between about 03 MLT and 23 MLT (duskward of which there is no scatter). Shortly afterwards, by 11:50 UT, the arc has brightened again (middle-left panel), but the arc then fades away again and by 14:02 UT it is not visible (bottom-left). It is during this period that the ionospheric flows in Figure 5 were observed (reproduced in Figure 6, middle-right). From 14:08 UT, there is further activity at 03 MLT, and the arc forms much more clearly than at any stage in the hours beforehand (e.g. 14:48 UT, bottom-right panel). Although the activity after 14:08 UT was identified as a separate arc from the activity which was present immediately after perigee, it is possible that this is merely a continuation of the earlier arc, but that the arc brightens and fades below the point at which it can easily be identified.

Three other arcs also occur after similar activity in the same local time sector:

- TPA 19 (1 February 2001, 12:46 UT) may be a continuation of an arc which was present as the spacecraft emerged from perigee at 10:50 UT (the location of which is consistent with ionospheric flows that were present between 10:10 and 10:50 UT), but which appeared to fade away by 12:00 UT.
- Prior to TPA 51 (8 January 2002, 18:26 UT), between 14:20 and 18:00 UT, there is intermittent activity in the dusk sector which includes features which could be identified as small polar cap arcs, but which were not included in the present survey as they were not separated distinctly enough from the main auroral oval to be identified as a clear TPA (e.g. Figure 7). However, before the formation of these features the level of ionospheric scatter in this local time is poor.
- In the case of TPA 111N (5 June 2004, 09:30 UT), the ionospheric flows are dawnward across the midnight sector, which is consistent with the formation mechanism, but they originate about one

hour of MLT duskward of the initial location of the arc (which is not consistent). The clarity of the images taken during this interval is relatively poor, and it is possible that the arc is a continuation of a very faint feature which was observed intermittently between the emergence from perigee (06:30 UT) and the time identified as the initial emergence of the arc. However, between the end of the perigee pass and 07:10 UT, there is no ionospheric scatter in the local time of the arc that is coincident with the main oval.

3.2.2 Radar geometry

The northern hemisphere ionospheric flows for TPA 123 are in the same direction across the midnight MLT sector as the reconnection mechanism would predict, but in the results of the map potential analysis the westward end of the flow channel appears to be close to 00 MLT rather than 21.5 MLT as would be expected from the location of the arc (Figure 5). On closer examination of the data that are used as an input to the map potential analysis (the line-of-sight component of the velocity), this appears to be a consequence of the radar geometry and the level of backscatter available. The results of the map potential technique for the period 11:00 to 11:10 UT on 1 June 2005 (which straddles the initial emergence of the arc at 11:04 UT) are replotted in Figure 8a, along with the fields of view of the three radars in the midnight sector at this time (King Salmon [KSR], Kodiak [KOD] and Prince George [PGR]). The line of sight velocity data from these three radars are plotted in Figure 8b & c. As the fields of view overlap, the backscatter data from the two poleward-pointing radars (KSR and KOD) are plotted in Figure 8b and the data from PGR (which points more westerly) are plotted in Figure 8c, but the fields of view of all three radars are overplotted in both panels. Most of the scatter is observed in the radars that point poleward, whereas PGR observed a limited patch of scatter indicating the presence of flows toward the radar immediately post-midnight (colored green – positive velocity components indicate flows towards the radar). The absence of scatter in the pre-midnight part of the PGR field of view means that there is no information on the dusk-dawn component of the ionospheric flow pre-midnight. The map potential plots in this paper show vectors that have been fitted to a solution for the distribution of the ionospheric electrostatic potential (indicated by contours in Figure 8a and all other map potential plots in this data); in regions without ionospheric data, the potential fit is constrained by data from a statistical model (*Ruohoniemi and Baker*, 1998). Therefore in the pre-midnight sector, the dusk/dawn components of the two dimensional map potential vectors are largely driven by the statistical model. Since the asymmetric azimuthal flows reported by *Grocott et al.* (2003) are only observed a small proportion of the time, their influence in the statistical model is weak. Consequently, the apparent MLT of the western end of the flow burst is unreliable in this case.

Finally in this section, we note that despite the fact that inconsistent flows were observed in all of the events in Figure 5, each event was preceded by a B_Y orientation that was consistent with the location of the arc at some point in the 3-5 hours preceding the arc.

3.3 Weak flows

In several other cases, the results of the map potential analysis indicated the presence of weak flows (< 200 m s^{-1}) coincident with the auroral oval and between the initial MLT of the arc and midnight MLT in the 30 minutes prior to the formation of the arc. In this section we examine directly the line-of-sight velocity data from radars in the midnight sector whose fields of view are coincident with the main auroral oval. As discussed in Section 3.2.2, it is important to consider the pointing direction of the radars, as the radar does not provide any information about velocities perpendicular to the beam directions. Therefore, we examined all of the events for which the map potential analysis indicated the presence of weak ionospheric flows on closed magnetic field lines in the midnight sector throughout the preceding 30 minutes, and discarded those for which the backscatter on which this was based was provided by radar beams which were mainly aligned poleward. Five events remain, which are listed in Table 2. All five occurred when the IMAGE satellite observed the transpolar arc in the northern hemisphere. Four of the events were selected because of the available ionospheric backscatter in the northern hemisphere, but TPA 3 was selected on the basis of the available backscatter in the southern hemisphere. There were no events where weak flows were observed in the midnight sector in both the northern and southern hemispheres.

The ionospheric data for these events are summarised in Figure 9. Each row shows the data from one event; the left-hand panel shows an auroral image taken a little while after the formation of the arc, indicating the local time at which it formed. The right-hand panel shows the field of view of the radar that is indicated in Table 2 and the line-of-sight velocity data observed by that radar at some point in the 30 minutes preceding the formation of the arc. An auroral image from the same time as the radar data is plotted underneath, in order to show the location of the auroral oval. The initial magnetic latitude and MLT (and uncertainty in the MLT) are indicated by a pink circle with error bars in both panels. The specific patch of backscatter that allows us to test the proposed formation mechanism is indicated by a red arrow.

In all five cases, the radars are situated on the same side of the midnight meridian as the initial MLT of the arc, and the equatorward beams of the radar have a component that is directed away from the initial location of the arc towards midnight MLT. In the cases of TPAs 3, 56 and 71, flows are observed away from the radar (indicated by negative velocity components, plotted in yellows/reds). This indicates the presence of flows across the midnight sector in a manner that is consistent with the *Milan et al.* (2005) mechanism and inconsistent with a symmetric Dungey cycle pattern.

In the cases of TPAs 29 and 79, moderate flows of order 200 m s^{-1} are observed towards the radar (positive velocity components, plotted in green). The line-of-sight components of the ionospheric flow therefore have a component directed from midnight MLT towards the initial location of the arc, and so appear to be inconsistent with the predictions of the *Milan et al.* (2005) mechanism and more comparable with symmetric Dungey cycle flows. In four of the five cases in Figure 9, a B_Y component that was consistent with the location of the arc was observed in the 3-5 hours before the arc was first observed. In the case of TPA 29N (an 'inconsistent' event), a continuously positive B_Y component was observed between 3 and 5 hours before the arc was observed, which is also inconsistent with the initial location that was identified for the arc.

4 Discussion

In this paper, we have examined the presence or absence of enhanced ionospheric flows preceding the formation of transpolar arcs, as predicted by *Milan et al.* (2005). Their mechanism predicts that transpolar arcs should be preceded by enhanced ionospheric flows on closed field lines in the midnight sector, which should start near the location at which the arc forms and be directed towards (and past) midnight MLT. For such flows to be observed, it is necessary for radar backscatter to be observed in the appropriate location. It was therefore necessary to identify those events for which there was a good level of backscatter across the midnight sector, at latitudes which correspond to newly-closed magnetic field lines (i.e. coincident with the main auroral oval). We examined the ionospheric data relating to 131 transpolar arcs that had previously been identified (*Fear and Milan*, 2012). As a first step, we identified those events for which there was backscatter coincident with the auroral oval between the initial MLT of the arc and midnight MLT in the 30 minutes preceding the first observation of the arc, and the fitted flow pattern from the map potential analysis (*Ruohoniemi and Baker*, 1998) exhibited a clear flow direction (with flows above 300 m s^{-1}). These criteria were satisfied in one hemisphere for 26 arcs, and in both hemispheres for a further arc. Considering the northern and southern hemispheres separately for the latter arc provides 28 independently-treated arcs. In 22 cases (79%), asymmetric flows were directed across midnight MLT and directed away from the initial MLT of the arc, and (where it is possible to determine from the level of backscatter) the channel of enhanced flow has a dawnward or duskward end that coincides well with the initial MLT of the arc.

The predicted flows at midnight MLT that precede transpolar arcs differ from the symmetric Dungey cycle convection cells (observed when the IMF is southward with $B_Y \approx 0$), but are consistent with asymmetric flows which are generally observed when the IMF has a significant B_Y component (e.g. *Ruohoniemi and Greenwald*, 2005). This is because regardless of the IMF orientation, any nightside asymmetry in the flow is caused by the IMF B_Y component that has been introduced into the magnetotail. However, statistical flow patterns derived for different IMF orientations show that the division between dawnward and duskward return flow is on average within about 1 hour of MLT from midnight (*Ruohoniemi and Greenwald*, 2005), whereas in case studies of the azimuthal flow bursts during intervals of northward IMF the difference has often been more extreme (*Grocott et al.*, 2003, 2004; *Milan et al.*, 2005). Furthermore, the *Milan et al.* (2005) mechanism specifically links the location of the division in the flow

with the location of the arc. In all of the events in Figure 2 (where the location of the dawnward or duskward end of the flow channel can be established), the edge of the flow channel matches the location at which the arc subsequently forms. In several of the events shown in Figure 4 (where the direction of the flow at midnight is consistent with the reconnection mechanism, but the precise location of the start of the flow channel cannot be established) the flow channel is observed to originate earlier than 23 MLT or later than 1 MLT, indicating that the flow channel originates more than an hour away from midnight (e.g. TPAs 23S, 34N, 34S, 64N, 66N). Therefore, we are confident that the azimuthal flows and transpolar arcs are directly linked rather than two independent effects with the same dependency on the IMF B_Y component. Indeed, although several of the previously-reported studies of azimuthal flows in the midnight sector have shown such flows originating two or more hours before/after midnight MLT, we have shown two events (TPAs 92N and 101N, Figure 2) where the arc and flow channel both originate within 1 hour of midnight MLT. Therefore, this formation mechanism appears to occur on a much less extreme scale too, and is clearly valid for arcs which form close to midnight.

In four of the apparently inconsistent cases with moderate or strong flows (discussed in Section 3.2.1), further examination of the auroral images reveals that the arc that was identified was preceded by similar activity in the same local time sector in the hours beforehand. In each case, there was no sign of an arc immediately before the formation time identified by *Fear and Milan* (2012) and listed in Table 1, and so the arc that was included in the survey was considered to be an independent event. Also in each case, the earlier activity was not identified as an additional arc because, when considered independently from the subsequent arc, it failed one of the three selection criteria applied by *Fear and Milan* (2012). Nonetheless, it is possible that the earlier activity is related to the arc that was included in the survey in these cases, and that they were identified as separate periods of activity due to a reduction in the intensity of the auroral emissions poleward of the main oval.

In one other case (Section 3.2.2), the cause of the apparent inconsistency was that the radar backscatter between the initial local time of the arc and 00 MLT was solely from radars with fields of view which were directed polewards and were therefore unable to return information about the east/west flows. It is therefore not possible to determine whether this event was consistent or inconsistent with the *Milan et al.* (2005) mechanism.

This just leaves one event (TPA 98) which was studied using the map potential technique and appears to be inconsistent with the mechanism but for which no satisfactory explanation has been found. The flows observed in the southern hemisphere at 04:00 UT (Figure 5) are directed dawnward at the local time of the arc, whereas the reconnection mechanism would predict duskward flows from the local time of the arc towards midnight. However, there is very little scatter between the duskward extent of the error bar (01 MLT) and midnight MLT. The initial MLT would have to have been identified erroneously (to a greater extent than the error bar would permit) for this event to be consistent with the reconnection mechanism, although the extra uncertainty in the initial MLT of this event would only have to be 0.5 hours of MLT for this to be the case.

The second stage of our analysis was to consider the events where the map potential analysis indicated that there was backscatter present between the initial location of the arc and midnight MLT (and coincident with the auroral oval), but that the flows were weak. In these cases, it is necessary to pay particular attention to the line-of-sight velocity data that are used by the map potential technique (Section 3.3). After discarding events where the velocity data in this sector was provided by radar beams which pointed predominantly poleward (i.e. where information about the azimuthal component of the flow was limited) we are left with five events. In three of these cases, the direction of the line-of-sight velocity component is consistent with the direction predicted by the *Milan et al.* (2005) mechanism, but in two cases it is inconsistent. In all cases in Figure 9, even the most equatorward radar beams have a poleward component to their pointing direction. The flows towards the radar prior to TPA 29 coincide with the initial location of the arc, and therefore may be due to the closure of flux in this local time sector. However, the backscatter prior to TPA 79 is situated duskward of the initial MLT of the arc; therefore even if the flows are mainly equatorward, rather than eastward, this is not consistent with the mechanism.

Combining the 'weak' and 'moderate or strong' flow events, asymmetric flows were directed across midnight MLT and directed away from the initial MLT of the arc in 25 cases (76%). In 12 of these cases, the dawnward or duskward edge of the flow channel was observed, and is consistent with the predicted location. Such a high proportion (combined with the consistent IMF dependence examined by *Fear and Milan* (2012)) provides strong support for the reconnection mechanism proposed by *Milan et al.* (2005).

We draw particular attention to the ionospheric flows observed preceding TPA 34. This event is unique in our survey in that there is a satisfactory level of backscatter coincident with the auroral oval in both hemispheres. The arc was observed by IMAGE whilst the satellite was above the northern hemisphere (TPA 34N in Figure 4), and the arc first emerged into the polar cap at 23:12 UT at 4.5 MLT. In the half hour beforehand, flows of order 500 m s^{-1} were observed duskward across midnight MLT, and coincident with the main auroral oval. Although there was no observation of the arc in the southern hemisphere, the auroral image was reversed about the midnight meridian for comparison with southern hemisphere data (TPA 34S). In the southern hemisphere, enhanced ionospheric flows of order 400 m s^{-1} were observed directed dawnward across midnight MLT and coincident with the oval. This illustrates the anti-conjugate nature of the reconnection-driven flows that precede the observable transpolar arc auroral emissions, consistent with the ionospheric flow observations discussed for magnetotail reconnection under northward IMF conditions by *Grocott et al.* (2003, 2004), and also consistent with the mechanism based on this process that was put forward by *Milan et al.* (2005).

Finally, we discuss the unusual evolution of TPA 50 (Figure 3) and its relationship to 'bending' arcs. *Kullen et al.* (2002) defined bending arcs as hook-shaped features which form with both ends attached to the main oval, where one end remains fixed to the main oval and the other swings out into the polar cap. Four of the 131 transpolar arcs identified by *Fear and Milan* (2012) were identified as bending arcs, and we speculated in that study that it is possible that they were formed by an alternative mechanism. This speculation arose from the observation that removing the 'bending' arcs improved the correlations that were observed between the IMF B_Y component and the local time at which the arcs formed. The arc plotted in Figure 3 (TPA 50) is one of the four bending arcs in our survey; as discussed in Section 3.1, the uncertainty on the initial MLT of this event is largely due to its formation process. This arc is visible as the distinct outlier with an initial MLT of 22 MLT and a large error bar ($\pm$3 hours) in Figures 5 & 7 of *Fear and Milan* (2012), and this event is the main cause of the reduced correlation coefficient when the bending arcs are included. Examination of Figure 3 in the present paper reveals that fast duskward flows are present in the midnight sector at 09:30 UT, which is 40 minutes before the time that was identified as the start time of the arc but only 20 minutes before the emergence of a feature at 01 MLT (visible at 09:50 UT in Figure 3) which could be interpreted as an embryonic TPA. Therefore, we suggest that the correct initial MLT is closer to 01 MLT than 22 MLT. Although this is within the error bar used in this study and by *Fear and Milan* (2012), it is not reflected in the correlation coefficients in our previous paper. Given the presence of consistent ionospheric flows at 09:30 UT, we conclude that this 'bending' arc is also consistent with the *Milan et al.* (2005) reconnection mechanism. Since the other bending arcs in Figure 7 of *Fear and Milan* (2012) had better-defined MLTs and were consistent with the trend of the non-bending arcs in that study, we believe that contrary to our earlier speculation there is no evidence to suggest that 'bending' arcs are formed by an alternative mechanism.

5 Conclusions

In this study, we have investigated whether transpolar arcs are preceded by asymmetric dawn/dusk ionospheric flows, as observed by the SuperDARN radar network, on closed magnetic field lines in the midnight sector. Such flows are predicted by the mechanism proposed by *Milan et al.* (2005), which is based on the premise that the arc is formed by reconnection in the magnetotail when the IMF is northward, but the magnetotail is twisted as a result of the recent time history of the IMF B_Y component. The presence or absence of these flows can only be investigated when there is sufficient backscatter in the midnight sector and coincident with the main auroral oval (indicating that the backscatter is on newly-closed magnetic field lines) in the $\sim$30 minutes preceding the initial emergence of the arc into the polar cap. These criteria was satisfied in 33 cases out of the 131 transpolar arcs that were identified by *Fear and Milan* (2012). In 25 cases, flows were observed that were consistent with the *Milan et al.* (2005) mechanism and (as far as could be determined from the available backscatter) had a dawnward or duskward extent that coincided with the initial MLT of the arc (as predicted by the mechanism). The flows observed before several of the apparently inconsistent events can be explained by either earlier activity in the same local time sector (indicating that the identified start time of the arc may be incorrect) or radar geometry. We conclude that the observations provide strong support for the transpolar arc formation mechanism proposed by *Milan et al.* (2005).

Acknowledgements

The authors were supported by STFC rolling grant ST/H002480/1. We are grateful to the SuperDARN PIs who provided the data used in this study. The IMAGE FUV data were provided by the NASA Space Science Data Center (NSSDC), and we gratefully acknowledge the PI of FUV, S. B. Mende of the University of California at Berkeley. We also express our gratitude to the referees.

References

Berkey, F. T., L. L. Cogger, S. Ismail, and Y. Kamide (1976), Evidence for a correlation between Sun-aligned arcs and the interplanetary magnetic field direction, *Geophys. Res. Lett.*, *3*(3), 145, doi:10.1029/GL003i003p00145.

Borovsky, J. E., R. J. Nemzek, and R. D. Belian (1993), The Occurrence Rate of Magnetospheric-Substorm Onsets: Random and Periodic Substorms, *J. Geophys. Res.*, *98*(A3), 3807–3813, doi:10.1029/92JA02556.

Carlson, H. C., and S. W. H. Cowley (2005), Accelerated polar rain electrons as the source of Sun-aligned arcs in the polar cap during northward interplanetary magnetic field conditions, *J. Geophys. Res.*, *110*(A5), 1–10, doi:10.1029/2004JA010669.

Chisham, G., M. Lester, S. E. Milan, M. P. Freeman, W. A. Bristow, A. Grocott, K. A. McWilliams, J. M. Ruohoniemi, T. K. Yeoman, P. L. Dyson, R. A. Greenwald, T. Kikuchi, M. Pinnock, J. P. S. Rash, N. Sato, G. J. Sofko, J.-P. Villain, and A. D. M. Walker (2007), A decade of the Super Dual Auroral Radar Network (SuperDARN): scientific achievements, new techniques and future directions, *Surv. Geophys.*, *28*, 33–109, doi:10.1007/s10712-007-9017-8.

Chiu, Y. T., N. U. Crooker, and D. J. Gorney (1985), Model of Oval and Polar Cap Arc Configurations, *J. Geophys. Res.*, *90*(A6), 5153–5157, doi:10.1029/JA090iA06p05153.

Cowley, S. W. H. (1981), Magnetospheric asymmetries associated with the Y-component of the IMF, *Planet. Space Sci.*, *29*, 79–96, doi:10.1016/0032-0633(81)90141-0.

Craven, J. D., J. S. Murphree, L. A. Frank, and L. L. Cogger (1991), Simultaneous optical observations of transpolar arcs in the two polar caps, *Geophys. Res. Lett.*, *18*(12), 2297–2300, doi:10.1029/91GL02308.

Cumnock, J. A., and L. G. Blomberg (2004), Transpolar arc evolution and associated potential patterns, *Ann. Geophys.*, *22*, 1213–1231, doi:10.5194/angeo-22-1213-2004.

Davis, T. N. (1963), Negative correlation between polar cap visual auroral and magnetic activity, *J. Geophys. Res.*, *68*(15), 4447–4453.

Dungey, J. W. (1961), Interplanetary Magnetic Field and the Auroral Zones, *Phys. Rev. Lett.*, *6*(2), 47–48, doi:10.1103/PhysRevLett.6.47.

Elphinstone, R. D., J. S. Murphree, D. J. Hearn, L. L. Cogger, I. Sandahl, P. T. Newell, D. M. Klumpar, S. Ohtani, J. A. Sauvaud, T. A. Potemra, K. Mursula, A. Wright, and M. Shapshak (1995), The Double Oval UV Auroral Distribution, 1. Implications for the Mapping of Auroral Arcs, *J. Geophys. Res.*, *100*(A7), 12,075–12,092, doi:10.1029/95JA00326.

Fairfield, D. H. (1979), On the Average Configuraton of the Geomagnetic Tail, *J. Geophys. Res.*, *84*(A5), 1950–1958, doi:10.1029/JA084iA05p01950.

Fear, R. C., and S. E. Milan (2012), The IMF dependence of the local time of transpolar arcs: Implications for formation mechanism, *J. Geophys. Res.*, *117*, A03213, doi:10.1029/2011JA017209.

Frank, L. A., J. D. Craven, J. L. Burch, and J. D. Winningham (1982), Polar views of the Earth's aurora with Dynamics Explorer, *Geophys. Res. Lett.*, *9*(9), 1001–1004, doi:10.1029/GL009i009p01001.

Frank, L. A., J. D. Craven, D. A. Gurnett, S. D. Shawhan, D. R. Weimer, J. L. Burch, J. D. Winningham, C. R. Chappell, J. H. Waite, R. A. Heelis, N. C. Maynard, M. Sugiura, W. K. Peterson, and E. G. Shelley (1986), The Theta Aurora, *J. Geophys. Res.*, *91*(A3), 3177–3224, doi:10.1029/JA091iA03p03177.

Goudarzi, A., M. Lester, S. E. Milan, and H. U. Frey (2008), Multi-instrumentation observations of a transpolar arc in the northern hemisphere, *Ann. Geophys.*, *26*, 201–210, doi:10.5194/angeo-26-201-2008.

Greenwald, R. A., K. B. Baker, J. R. Dudeney, M. Pinnock, T. B. Jones, E. C. Thomas, J. P. Villain, J. C. Cerisier, C. Senior, C. Hanuise, R. D. Hunsucker, G. Sofko, J. Koehler, E. Nielsen, R. Pellinen, A. D. M. Walker, N. Sato, and H. Yamagishi (1995), DARN/SuperDARN: A global view of high-latitude convection, *Space Sci. Rev.*, *71*, 761–796, doi:10.1007/BF00751350.

Grocott, A., S. W. H. Cowley, and J. B. Sigwarth (2003), Ionospheric flow during extended intervals of northward but B_Y-dominated IMF, *Ann. Geophys.*, *21*(2), 509–538, doi:10.5194/angeo-21-509-2003.

Grocott, A., S. V. Badman, S. W. H. Cowley, T. K. Yeoman, and P. J. Cripps (2004), The influence of IMF B_Y on the nature of the nightside high-latitude ionospheric flow during intervals of positive IMF B_Z, *Ann. Geophys.*, *22*(5), 1755–1764, doi:10.5194/angeo-22-1755-2004.

Gusev, M. G., and O. A. Troshichev (1986), Hook-shaped arcs in dayside polar cap and their relation to the IMF, *Planet. Space Sci.*, *34*(6), 489–496, doi:10.1016/0032-0633(86)90087-5.

Gussenhoven, M. S. (1982), Extremely High Latitude Auroras, *J. Geophys. Res.*, *87*(A4), 2401–2412, doi:10.1029/JA087iA04p02401.

Hosokawa, K., J. I. Moen, K. Shiokawa, and Y. Otsuka (2011), Motion of polar cap arcs, *J. Geophys. Res.*, *116*, A01305, doi:10.1029/2010JA015906.

King, J. H., and N. E. Papitashvili (2005), Solar wind spatial scales in and comparisons of hourly Wind and ACE plasma and magnetic field data, *J. Geophys. Res.*, *110*, A02104, doi:10.1029/2004JA010649.

Kullen, A. (2000), The connection between transpolar arcs and magnetotail rotation, *Geophys. Res. Lett.*, *27*(1), 73–76, doi:10.1029/1999GL010675.

Kullen, A., M. Brittnacher, J. A. Cumnock, and L. G. Blomberg (2002), Solar wind dependence of the occurrence and motion of polar auroral arcs: A statistical study, *J. Geophys. Res.*, *107*(A11), 1326, doi:10.1029/2002JA009245.

Liou, K., J. M. Ruohoniemi, P. T. Newell, R. Greenwald, C.-I. Meng, and M. R. Hairston (2005), Observations of ionospheric plasma flows within theta auroras, *J. Geophys. Res.*, *110*, A03303, doi:10.1029/2004JA010735.

Lyons, L. R. (1985), A Simple Model for Polar Cap Convection Patterns and Generation of θ Auroras, *J. Geophys. Res.*, *90*(A2), 1561–1567, doi:10.1029/JA090iA02p01561.

Makita, K., C.-I. Meng, and S.-I. Akasofu (1991), Transpolar Auroras, Their Particle Precipitation, and IMF B_Y Component, *J. Geophys. Res.*, *96*(A8), 14,085–14,095, doi:10.1029/90JA02323.

Mawson, D. (1925), Records of the Aurora Polaris, *Australasian Antarctic Expedition 1911-14, Scientific Reports Series B.*

Mende, S. B., H. Heetderks, H. U. Frey, M. Lampton, S. P. Geller, S. Habraken, E. Renotte, C. Jamar, P. Rochus, J. Spann, S. A. Fuselier, J.-C. Gerard, R. Gladstone, S. Murphree, and L. Cogger (2000a), Far Ultraviolet Imaging from the IMAGE Spacecraft: 1. System Design, *Space Sci. Rev.*, *91*, 243–270, doi:10.1023/A:1005271728567.

Mende, S. B., H. Heetderks, H. U. Frey, M. Lampton, S. P. Geller, R. Abiad, O. H. W. Siegmund, A. S. Tremsin, J. Spann, H. Dougani, S. A. Fuselier, A. L. Magoncelli, M. B. Bumala, S. Murphree, and T. Trondsen (2000b), Far Ultraviolet Imaging from the IMAGE Spacecraft: 2. Wideband FUV Imaging, *Space Sci. Rev.*, *91*, 271–285, doi:10.1023/A:1005227915363.

Mende, S. B., H. Heetderks, H. U. Frey, J. M. Stock, M. Lampton, S. P. Geller, R. Abiad, O. H. W. Siegmund, S. Habraken, E. Renotte, C. Jamar, P. Rochus, J.-C. Gerard, R. Sigler, and H. Lauche (2000c), Far Ultraviolet Imaging from the IMAGE Spacecraft: 3. Spectral Imaging of Lyman-α and OI 135.6nm, *Space Sci. Rev.*, *91*, 287–318, doi:10.1023/A:1005292301251.

Milan, S. E. (2004), A simple model of the flux content of the distant magnetotail, *J. Geophys. Res.*, *109*, A07210, doi:10.1029/2004JA010397.

Milan, S. E., B. Hubert, and A. Grocott (2005), Formation and motion of a transpolar arc in response to dayside and nightside reconnection, *J. Geophys. Res.*, *110*, A01212, doi:10.1029/2004JA010835.

Milan, S. E., G. Provan, and B. Hubert (2007), Magnetic flux transport in the Dungey cycle: A survey of dayside and nightside reconnection rates, *J. Geophys. Res.*, *112*, A01209, doi:10.1029/2006JA011642.

Nielsen, E., J. D. Craven, L. A. Frank, and R. A. Heelis (1990), Ionospheric Flows Associated With a Transpolar Arc, *J. Geophys. Res.*, *95*(A12), 21,169–21,178, doi:10.1029/JA095iA12p21169.

Østgaard, N., S. B. Mende, H. U. Frey, L. A. Frank, and J. B. Sigwarth (2003), Observations of non-conjugate theta aurora, *Geophys. Res. Lett.*, *30*(21), 2125, doi:10.1029/2003GL017914.

Peterson, W. K., and E. G. Shelley (1984), Origin of the Plasma in a Cross-Polar Cap Auroral Feature (Theta Aurora), *J. Geophys. Res.*, *89*(A8), 6729–6736, doi:10.1029/JA089iA08p06729.

Reiff, P. H., and J. L. Burch (1985), IMF B_Y-Dependent Plasma Flow and Birkeland Currents in the Dayside Magnetosphere, 2. A Global Model for Northward and Southward IMF, *J. Geophys. Res.*, *90*(A2), 1595–1609, doi:10.1029/JA090iA02p01595.

Rezhenov, B. V. (1995), A possible mechanism for θ aurora formation, *Ann. Geophys.*, *13*(7), 698–703, doi:10.1007/s00585-995-0698-3.

Ruohoniemi, J. M., and K. B. Baker (1998), Large-scale imaging of high-latitude convection with Super Dual Auroral Radar Network HF radar observations, *J. Geophys. Res.*, *103*(A9), 20,797–20,811, doi:10.1029/98JA01288.

Ruohoniemi, J. M., and R. A. Greenwald (2005), Dependencies of high-latitude plasma convection: Consideration of interplanetary magnetic field, seasonal, and universal time factors in statistical patterns, *J. Geophys. Res.*, *110*, A09204, doi:10.1029/2004JA010815.

Russell, C. T. (1972), The configuration of the magnetosphere, in *Critical Problems of Magnetospheric Physics*, edited by E. R. Dyer, pp. 1–16, National Academy of Science, Washington D. C.

Senior, C., J.-C. Cerisier, F. Rich, M. Lester, and G. K. Parks (2002), Strong sunward propagating flow bursts in the night sector during quiet solar wind conditions: SuperDARN and satellite observations, *Ann. Geophys.*, *20*, 771–779.

Shinohara, I., and S. Kokubun (1996), Statistical properties of particle precipitation in the polar cap during intervals of northward interplanetary magnetic field, *J. Geophys. Res.*, *101*(A1), 69–82, doi:10.1029/95JA01848.

Tsyganenko, N. A. (1989), A magnetospheric magnetic field model with a warped tail current sheet, *Planet. Space Sci.*, *37*(1), 5–20, doi:10.1016/0032-0633(89)90066-4.

Valladares, C. E., H. C. Carlson, and K. Fukui (1994), Interplanetary Magnetic Field Dependency of Stable Sun-Aligned Polar Cap Arcs, *J. Geophys. Res.*, *99*(A4), 6247–6272, doi:10.1029/93JA03255.

Weill, G. (1958), Aspects de l'aurore observée à la base Dumont-d'Urville en Terre Adélie, *C. R. Acad. Sci.*, *246*(2), 2925–2927.

Zhu, L., R. W. Schunk, and J. J. Sojka (1997), Polar cap arcs: a review, *J. Atmos. Sol.-Terr. Phy.*, *59*(10), 1087–1126, doi:10.1016/S1364-6826(96)00113-7.

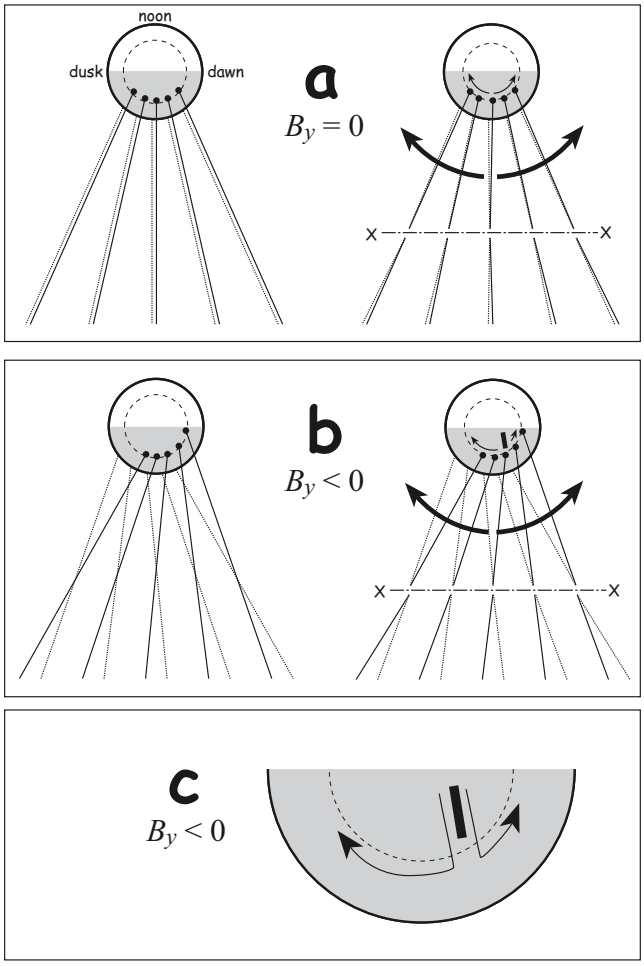

Figure 1: A cartoon illustrating the *Milan et al.* (2005) mechanism for the formation of transpolar arcs. The top two panels show a view of magnetotail reconnection when the B_Y component in the magnetotail is (a) approximately zero and (b) negative. In case (a), newly-closed flux returns to the dayside as envisaged by *Dungey* (1961). In case (b), the magnetotail is twisted, asymmetric azimuthal flows are expected in the midnight sector (*Grocott et al.*, 2003, 2004) and a transpolar arc is formed near the footprint of the field line which crosses the magnetic equator at midnight MLT. This location (indicated by the black rectangle) is also expected to be the start point of the asymmetric azimuthal flow. The flows observed in (b) are enlarged in panel (c). (After *Milan et al.* (2005).)

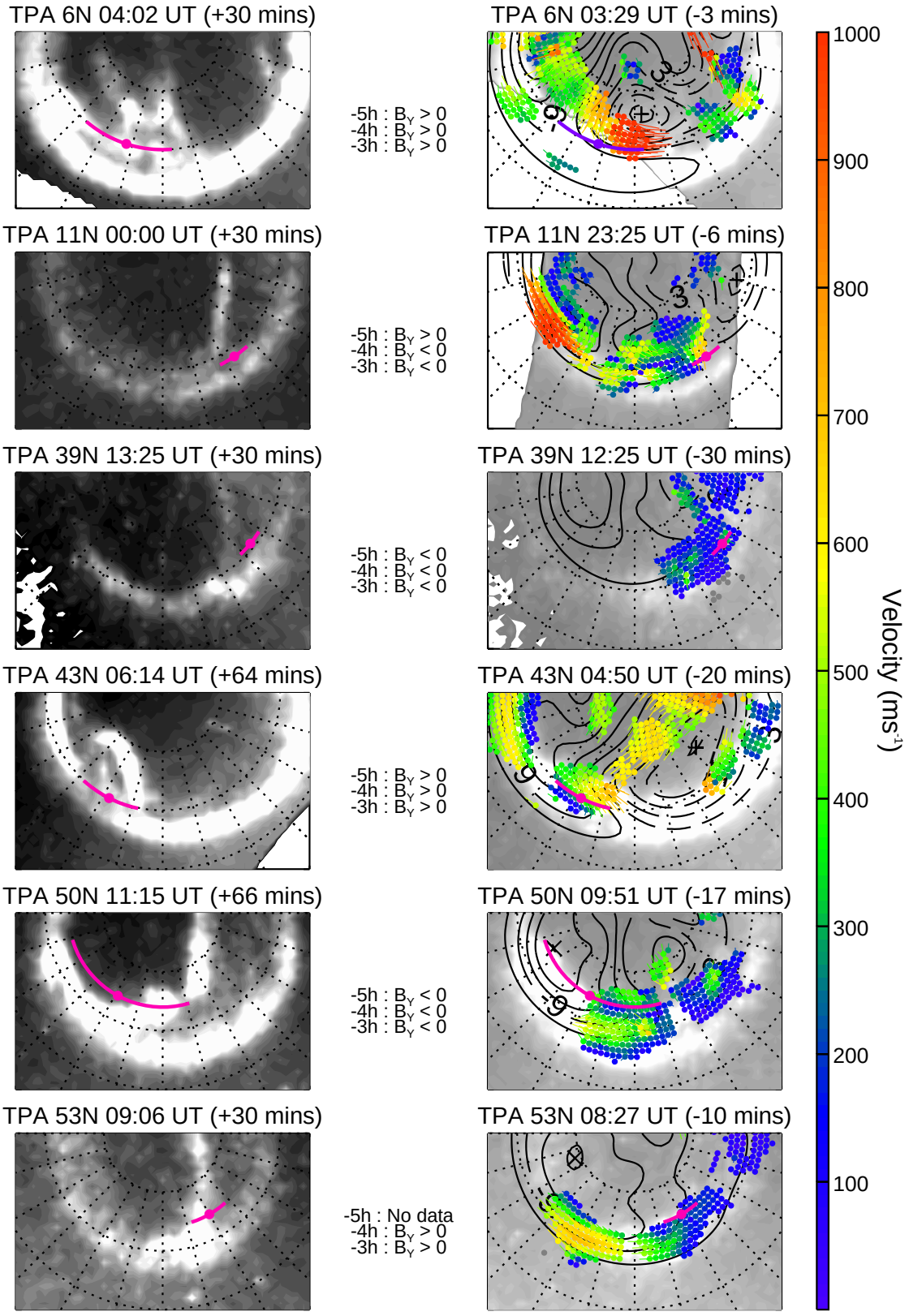

Figure 2: Events with a flow channel with a consistent flow direction and a dawnward/duskward edge that is consistent with the *Milan et al.* (2005) mechanism. The left-hand column shows an auroral image taken after the formation of the arc. The right-hand column shows an auroral image before the arc formed (black & white), and the ionospheric flows observed at the same time as the corresponding image (color). In cases where an image is compared with ionospheric data from the opposite hemisphere, the auroral image is mirrored about the midnight meridian. The central figures indicate the sign of the IMF B_Y component in one-hour blocks centred 3, 4 and 5 hours before the TPA was first observed. (Figure continues overleaf.)

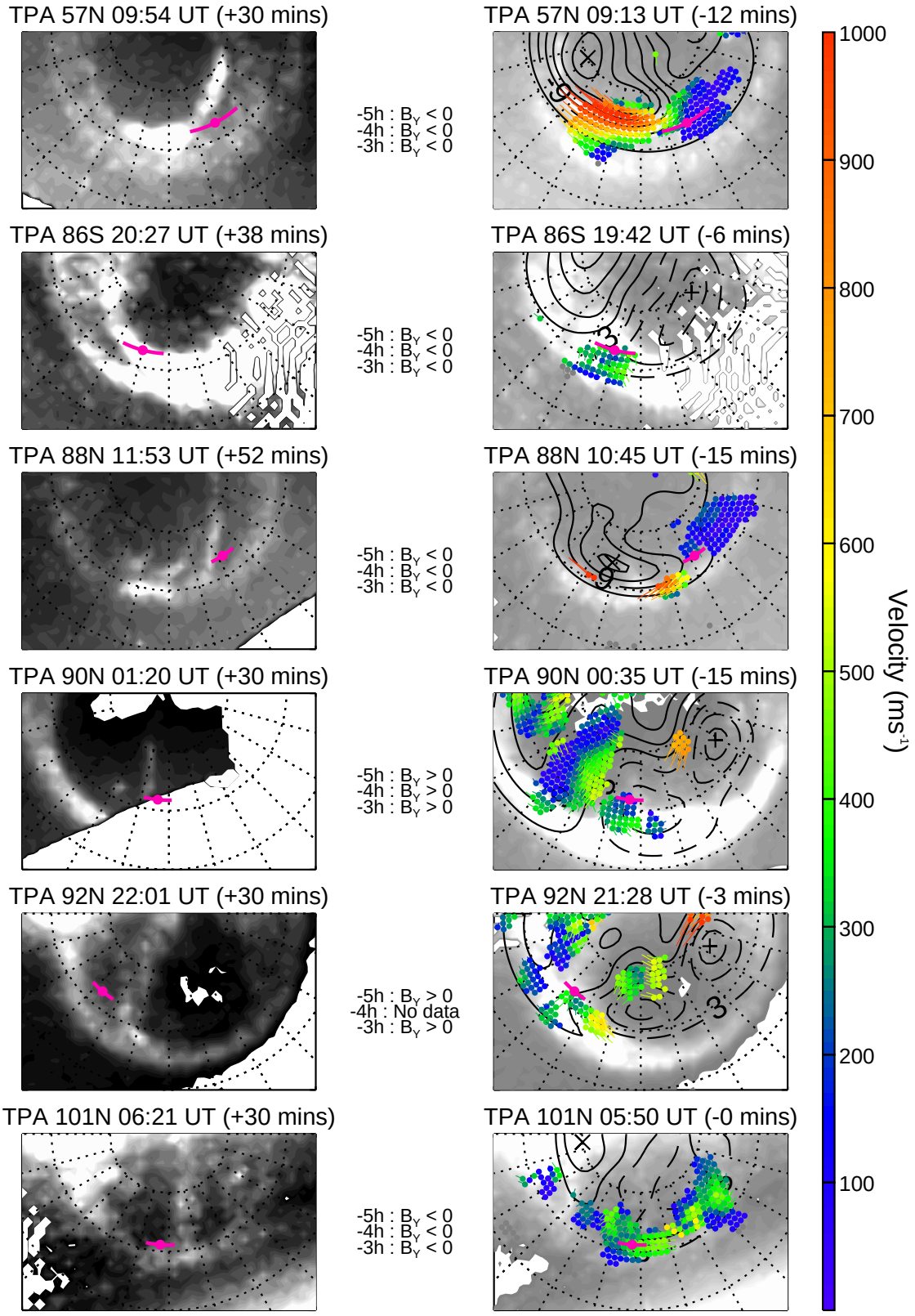

Figure 2 continued

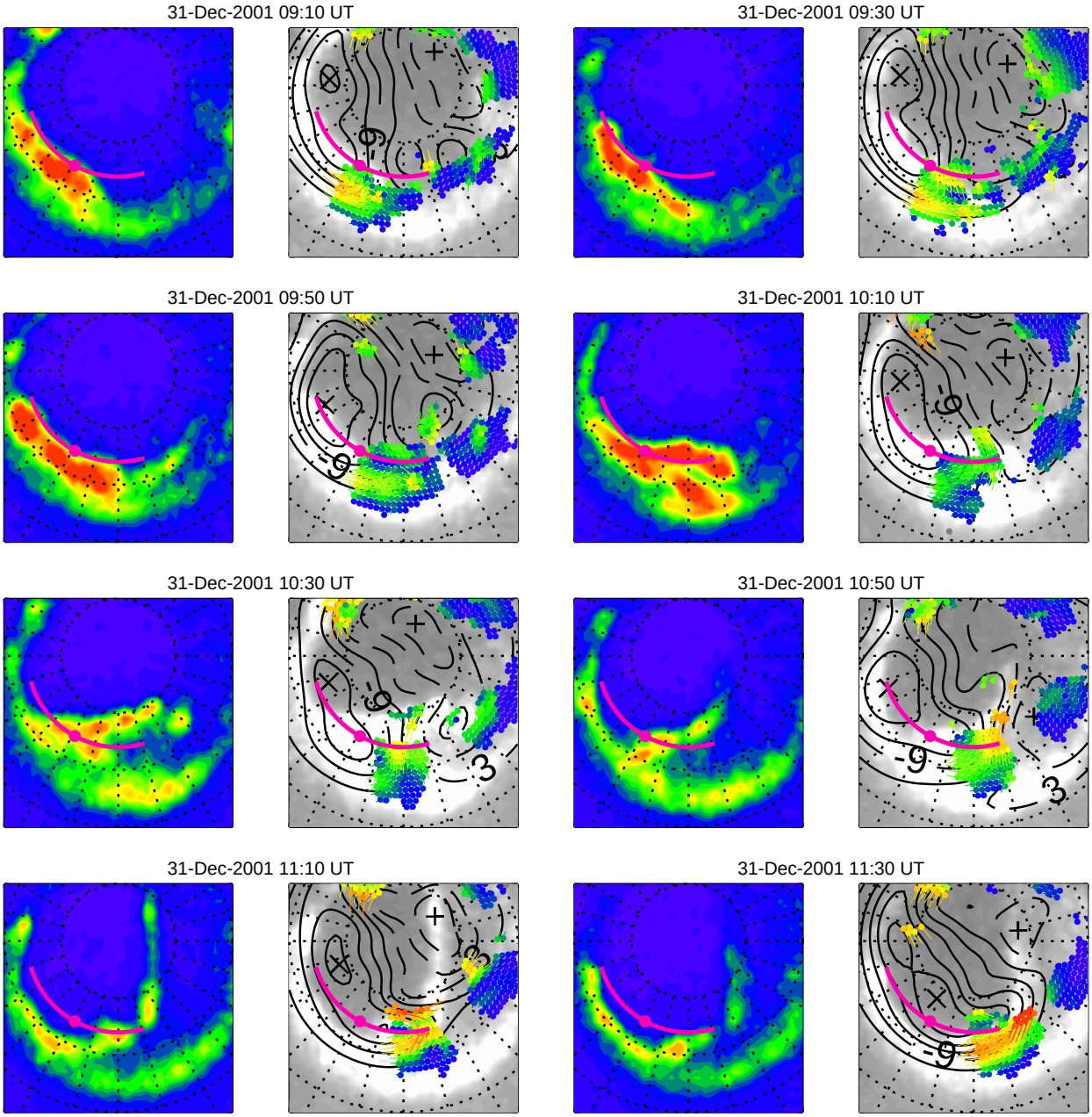

Figure 3: A series of auroral images and ionospheric flow patterns showing the uncharacteristic development of TPA 50. Each pair of images contains data from the same period (indicated above each pair of plots). The black and white images show the same image as the color plot on its left, but are overlain by ionospheric flow vectors derived by the map potential technique. The central value of the initial local time of the arc (22 MLT) was identified from the feature that is observed forming at 10:10 and 10:30 UT, and the uncertainty (±3 hours of MLT) was selected so that the feature which is observed developing at 01 MLT at 09:50 UT and the main protrusion of the arc into the polar cap at 11:10 UT (also at 01 MLT) were included. This arc resembles the 'bending' arcs described by *Kullen et al.* (2002).

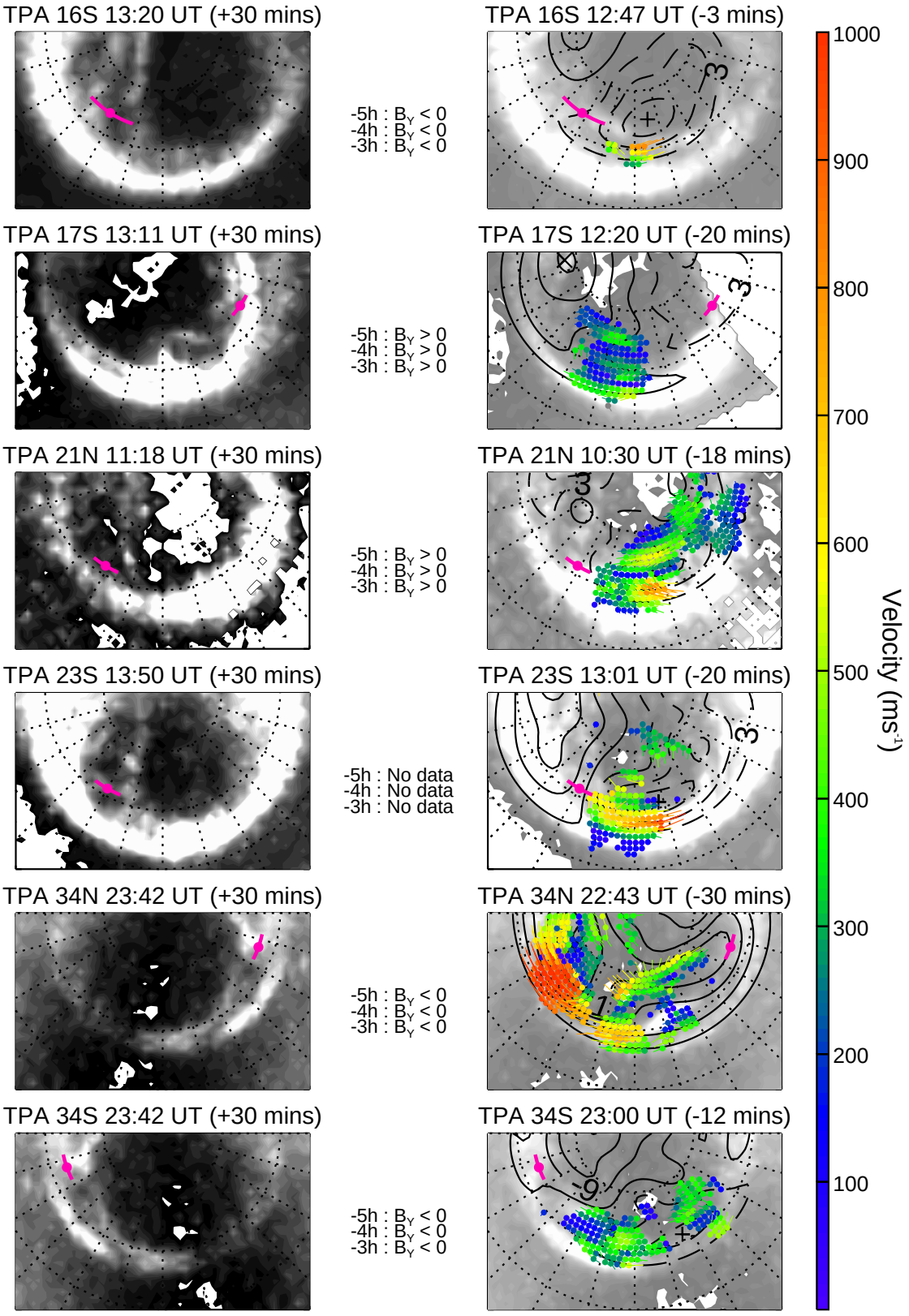

Figure 4: Events where there is insufficient scatter to identify the dawnward/duskward edge of the flow channel, but where there are flows in the midnight sector, or between the initial MLT of the arc and midnight MLT, that are consistent with the *Milan et al.* (2005) mechanism. This figure adopts the same format as Figure 2.

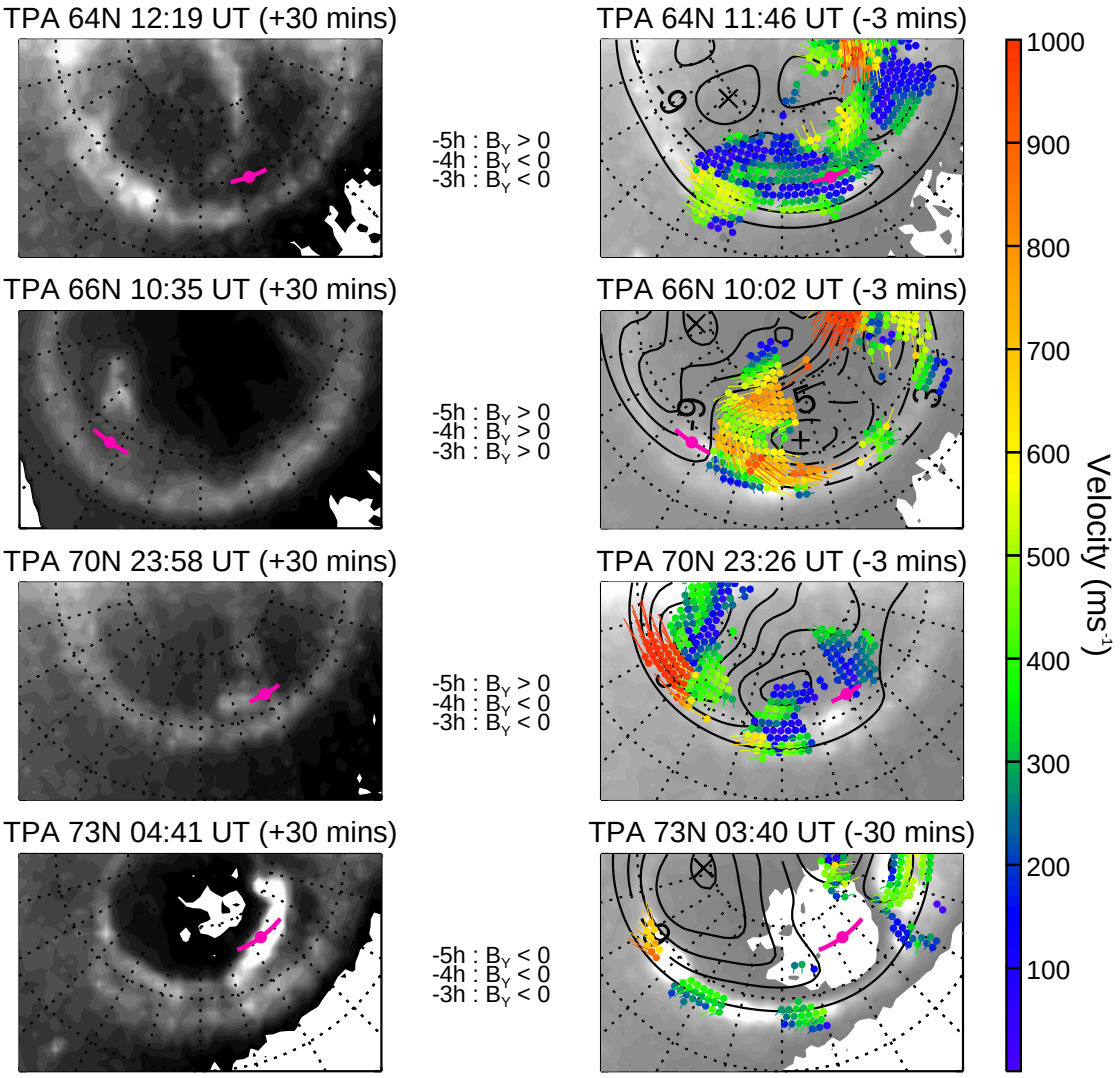

Figure 4 continued

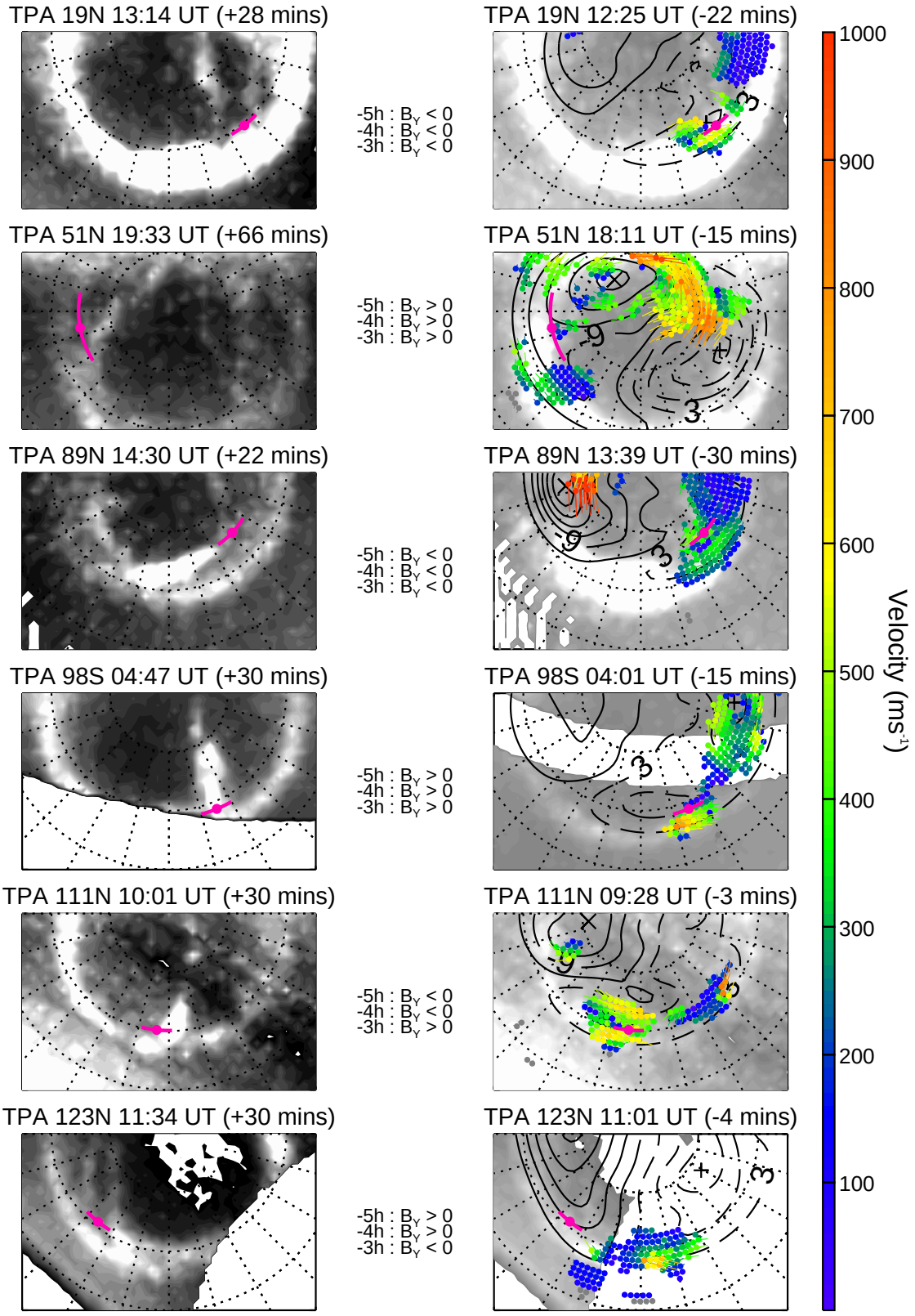

Figure 5: Events with flows which appear to be inconsistent with the *Milan et al.* (2005) mechanism. This figure adopts the same format as Figure 2.

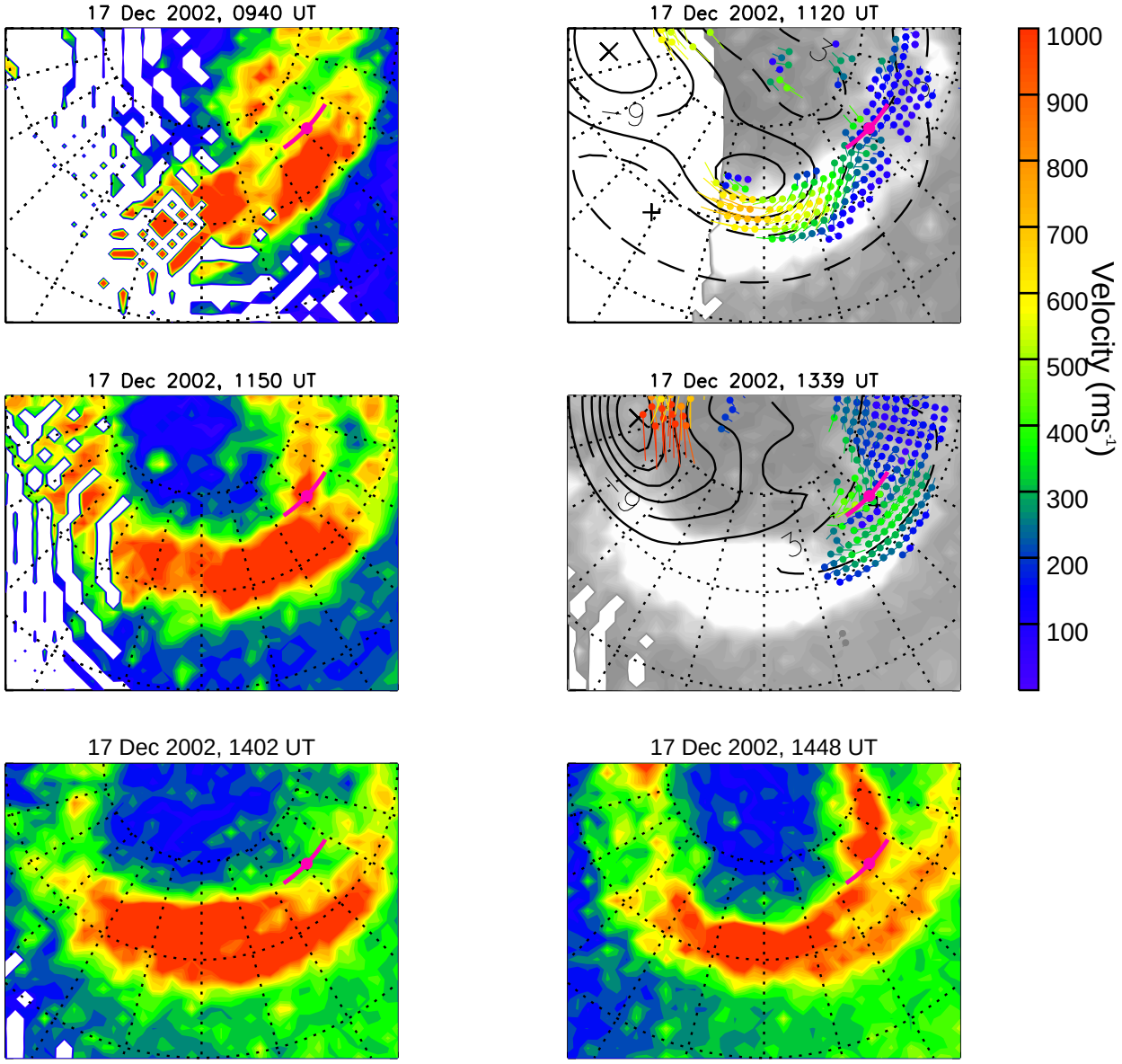

Figure 6: The evolution of TPA 89. Each panel shows an auroral image and/or map potential data from a period within the 5 hours prior to the formation of the arc at 14:08 UT. The developed arc is observed in the bottom-right panel at 14:48 UT. No arc was visible in the same local time sector at 14:02 (bottom left), but there is evidence of earlier activity in the same local time sector (top and middle rows).

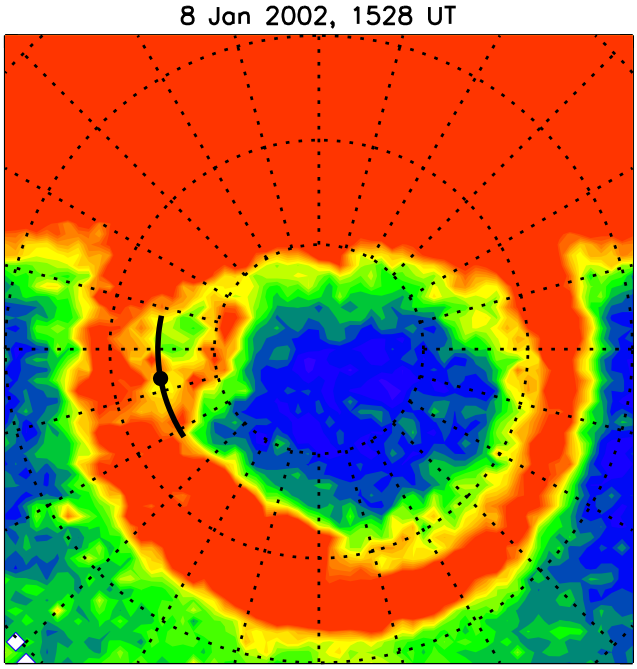

Figure 7: An image of the polar cap about three hours before the formation of TPA 51. A potential arc (which is not distinct enough from the main oval to be identified as a TPA in this survey) is present at the same local time sector as the later formation of the arc (∼20 MLT).

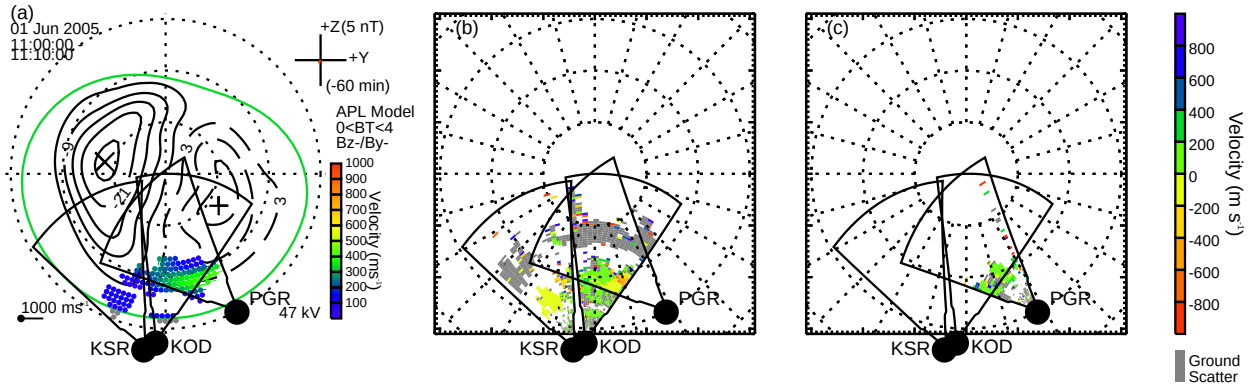

Figure 8: (a) The two dimensional vectors produced from the map potential routine at the same time as the formation of TPA 123, overlaid by the fields of view of the King Salmon, Kodiak and Prince George radars (KSR, KOD & PGR). (b) The line of sight velocity data from the two poleward-pointing radars (KSR & KOD), with the field of view of PGR also shown. (c) The line of sight velocity data from the only azimuthally-directed radar in this time sector (PGR), with the fields of view of KSR & KOD also shown.

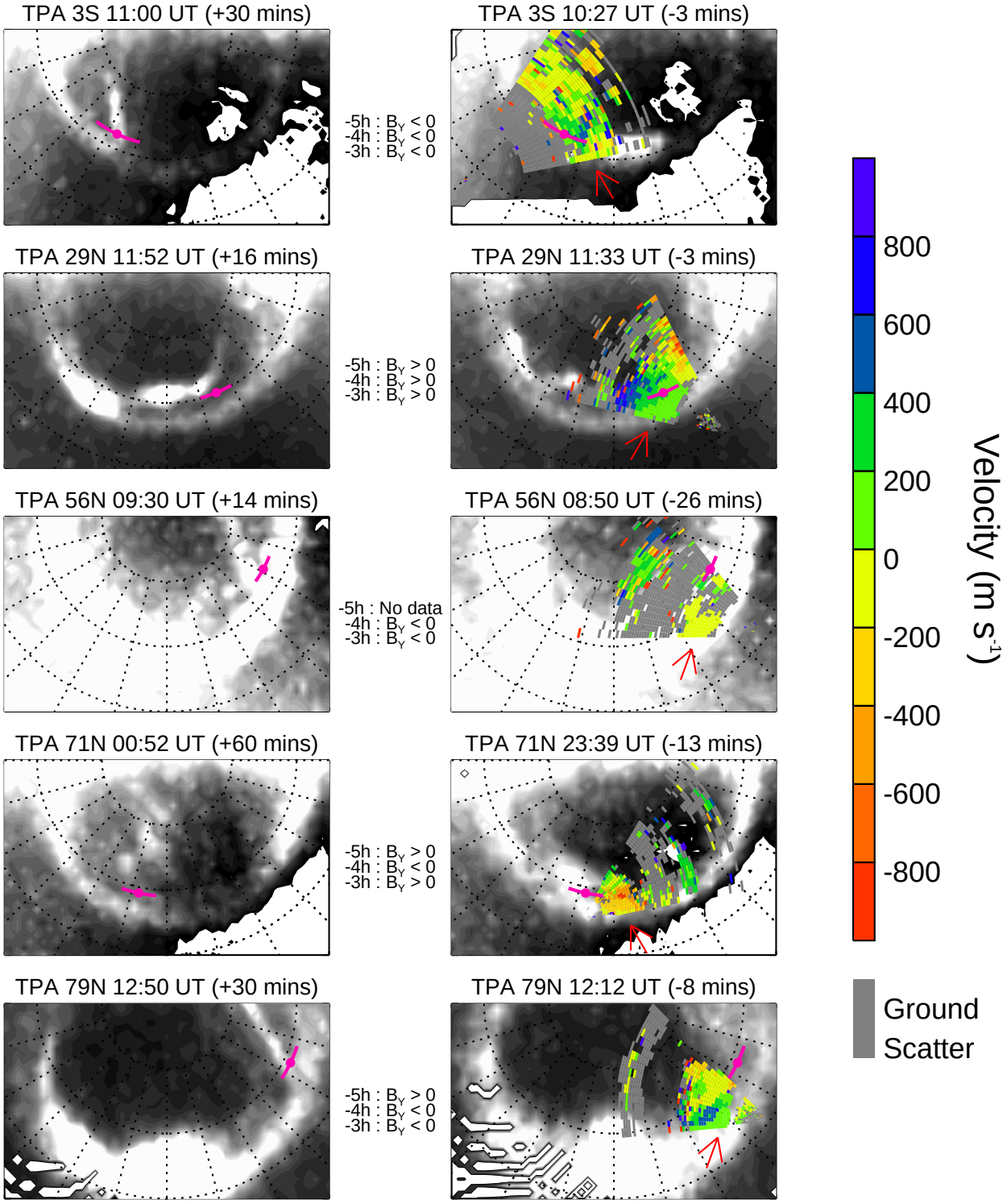

Figure 9: Events for which weak flows are evident in the results of the map potential analysis (listed in Table 2). The left-hand column shows an auroral image taken after the formation of the arc. The right-hand column shows an auroral image before the arc formed (black & white), and the line-of-sight velocity data from the radar indicated in Table 2 (color). The patch of backscatter that is of interest is highlighted by a red arrow. In the case of TPA 3, the auroral image is mirrored about the midnight meridian as a northern hemisphere image is being compared with southern hemisphere velocity data. The central figures indicate the sign of the IMF B_Y component in one-hour blocks centred 3, 4 and 5 hours before the TPA was first observed.

TPA no.	Start time (UT)	NH scatter	SH scatter	IMAGE hemisphere
6	05-Nov-2000 03:32 UT	✓		N
11	27-Dec-2000 23:30 UT	✓		N
16	22-Jan-2001 12:50 UT		✓	N
17	29-Jan-2001 12:40 UT		✓	N
19	01-Feb-2001 12:46 UT	✓		N
21	12-Feb-2001 10:48 UT	✓		N
23	20-Feb-2001 13:20 UT		✓	N
34	18-Oct-2001 23:12 UT	✓	✓	N
39	08-Nov-2001 12:54 UT	✓		N
43	18-Nov-2001 05:10 UT	✓		N
50	31-Dec-2001 10:08 UT	✓		N
51	08-Jan-2002 18:26 UT	✓		N
53	19-Jan-2002 08:36 UT	✓		N
57	28-Jan-2002 09:24 UT	✓		N
64	02-Mar-2002 11:48 UT	✓		N
66	04-Mar-2002 10:04 UT	✓		N
70	11-Mar-2002 23:28 UT	✓		N
73	25-Mar-2002 04:10 UT	✓		N
86	09-Dec-2002 19:48 UT		✓	N
88	13-Dec-2002 11:00 UT	✓		N
89	17-Dec-2002 14:08 UT	✓		N
90	20-Dec-2002 00:50 UT	✓		N
92	14-Feb-2003 21:30 UT	✓		N
98	14-Mar-2003 04:16 UT		✓	N
101	22-Jul-2003 05:50 UT	✓		S
111	05-Jun-2004 09:30 UT	✓		S
123	01-Jun-2005 11:04 UT	✓		S

Table 1: Transpolar arcs identified by *Fear and Milan* (2012) which have ionospheric scatter coincident with the main auroral oval that is sufficient to identify whether the formation of the arc is consistent with the *Milan et al.* (2005) mechanism.

TPA no.	Start time (UT)	NH scatter	SH scatter	IMAGE hemisphere
3	23-Sep-2000 10:30 UT		TIG	N
29	08-Mar-2001 11:36 UT	PGR		N
56	25-Jan-2002 09:16 UT	KAP		N
71	15-Mar-2002 23:52 UT	PYK		N
79	30-Oct-2002 12:20 UT	PGR		N

Table 2: Transpolar arcs identified by *Fear and Milan* (2012) which have ionospheric scatter coincident with the main auroral oval which the map potential analysis indicates are weak flows. The radar in which the scatter is present is indicated (TIG: Tiger, PGR: Prince George, KAP: Kapuskasing, PYK: Þikvibær). The line-of-sight data from the radars indicated in this table are analysed further in Figure 9.